

1 **Evaluation of eleven terrestrial carbon-nitrogen cycle models**
2 **against observations from two temperate Free-Air CO₂ Enrichment Studies**

3

4 Zaehle, Sönke (1*), Medlyn, Belinda E. (2), De Kauwe, Martin G. (2), Walker, Anthony P. (3),
5 Dietze, Michael C. (4), Hickler, Thomas (5), Luo, Yiqi (6), Wang, Ying-Ping (7),
6 El-Masri, Bassil (8), Thornton, Peter (3), Jain, Atul, (8), Wang, Shusen (9), Warlind, David (10),
7 Weng, Ensheng (11), Parton, William (12), Iversen, Colleen M. (3), Gallet-Budynek, Anne (13),
8 McCarthy, Heather (6), Finzi, Adrien (14), Hanson, Paul J. (3), Prentice, I Colin (2,15),
9 Oren, Ram (16), Norby, Richard J (3)

10

11 1) Biogeochemical Integration Department, Max Planck Institute for Biogeochemistry, Hans-Knöll-
12 Str. 10, D-07745 Jena, Germany (Tel: +49-3641-57-6325, email: szaehle@bgc-jena.mpg.de).

13 2) Department of Biological Science, Macquarie University, Sydney, NSW 2109, Australia

14 3) Oak Ridge National Laboratory, Environmental Sciences Division and Climate Change Science
15 Institute, Oak Ridge, TN 37831, USA

16 4) Department of Earth and Environment, Boston University, Boston, MA 02215, USA

17 5) Biodiversity and Climate Research Centre (BiK-F) & Senckenberg Gesellschaft für
18 Naturforschung, & Department of Physical Geography, Goethe University, D-60438 Frankfurt
19 am Main, Germany.

20 6) Department of Microbiology & Plant Biology, University of Oklahoma, Norman, OK 73019,
21 USA

22 7) CSIRO Marine and Atmospheric Research, PMB 1, Aspendale, Victoria 3195, Australia

23 8) Department of Atmospheric Sciences, University of Illinois, Urbana, IL 61801, USA

24 9) Natural Resources Canada, Ottawa, ON, Canada

25 10) Department of Physical Geography and Ecosystem Science, Lund University, Lund,
26 Sweden

27 11) Department of Ecology and Evolutionary Biology, Princeton University
28 Princeton, NJ 08544

29 12) Natural Resource Ecology Laboratory, Colorado State University, Fort Collins, CO 80523,
30 USA.

- 31 13) INRA, UMR1220 TCEM, F-33882 Villenave d'Ornon & Univ. Bordeaux, UMR1220
32 TCEM, F-33175 Gradignan, France
- 33 14) Department of Biology, Boston University, Boston, MA 02215, USA
- 34 15) AXA Chair of Biosphere and Climate Impacts, Department of Life Sciences and Grantham
35 Institute for Climate Change, Imperial College London, Silwood Park, Ascot SL5 7PY, UK
- 36 16) Division of Environmental Science & Policy, Nicholas School of the Environment, Duke
37 University, Durham, NC 27708 & Department of Forest Ecology & Management, Swedish
38 University of Agricultural Sciences (SLU), SE-901 83, Umeå, Sweden

39 *) Corresponding author

40

41

42 **Total length: 9519**

43 Summary: 214

44 Introduction: 863

45 Methods: 1864

46 Results: 3457

47 Discussion: 2458

48 Conclusions: 868

49 Acknowledgements: 140

50 9 figures, 1 supplementary figure, 2 Appendix-Tables

51

52 **Summary**

- 53 • We analysed the responses of 11 ecosystem models to elevated atmospheric [CO₂] (eCO₂) at two
54 temperate forest ecosystems (Duke and ORNL Free-Air CO₂ Enrichment (FACE) experiments)
55 to test alternative representations of carbon-nitrogen cycle processes.
- 56 • We decomposed the model responses into component processes affecting the response to eCO₂
57 and confronted these with observations from the FACE experiments.
- 58 • Most of the models reproduced the observed initial enhancement of NPP at both sites, but none
59 was able to simulate both, the sustained 10-year enhancement at Duke and the declining
60 response at ORNL: models generally showed signs of progressive nitrogen limitation due to
61 lower-than-observed plant nitrogen uptake. Nonetheless, many models showed qualitative
62 agreement with observed component processes. The results suggest that improved representation
63 of above-belowground interactions and better constraints on plant stoichiometry are important
64 for a predictive understanding of eCO₂ effects. Improved accuracy of soil organic matter
65 inventories are pivotal to reduce uncertainty in observed C-N budgets.
- 66 • The two FACE experiments are insufficient to fully constrain terrestrial responses to eCO₂.
67 given the complexity of factors leading to the observed diverging trends, and the consequential
68 inability of the models to explain these trends. Nevertheless, the ecosystem models were able to
69 capture important features of the experiments, lending some support to their projections.

70

71 Keywords: CO₂ fertilisation, elevated CO₂, FACE, nitrogen limitation, carbon storage, plant
72 physiology, ecosystem modelling, model evaluation

73

74 **1. Introduction**

75 Rising atmospheric [CO_2] from anthropogenic fossil fuel emissions fertilises plants (Liebig, 1843;
76 Arrhenius, 1896; Ainsworth & Long, 2005). Biosphere models integrating the effects of [CO_2] on
77 plant photosynthesis into projections of the global terrestrial carbon (C) balance suggest that
78 elevated atmospheric [CO_2] (eCO_2) has caused a large fraction of the land C sequestration during
79 recent decades (Cramer *et al.*, 2001; Sitch *et al.*, 2013). These models also project that the CO_2 -
80 induced land C sequestration will continue in the future and thereby significantly reduce the
81 accumulation rate of anthropogenic CO_2 in the atmosphere (Arora *et al.*, 2013). However, most of
82 these models do not account for the limited availability of nitrogen (N) for plant uptake and growth
83 in many terrestrial ecosystems (Vitousek & Howarth, 1991), which could attenuate ecosystem C
84 storage in response to eCO_2 : increased C sequestration due to eCO_2 is thought to bind N into less
85 easily available forms of N within a few years after the onset of CO_2 fertilisation, a process referred
86 to as progressive N limitation (PNL, Comins & McMurtrie, 1993; Luo *et al.*, 2004). Terrestrial
87 biosphere models that explicitly consider the carbon-nitrogen cycle interaction show that future
88 land C sequestration could be reduced by 50% or more because of N cycle processes (Sokolov *et*
89 *al.*, 2008; Thornton *et al.*, 2009; Zaehle *et al.*, 2010). However, estimates of the magnitude of this N
90 effect differ strongly among these projections as a result of uncertainty in the representation of key
91 processes determining the strength of the N constraint on land C storage (Zaehle & Dalmonech,
92 2011).

93 Free-Air CO_2 Enrichment (FACE) experiments in N-limited temperate forest ecosystems provide a
94 unique source of empirical evidence for the ecosystem-scale response of the interacting C and N
95 cycle processes to eCO_2 (Oren *et al.*, 2001; Norby *et al.*, 2005; Palmroth *et al.*, 2006; Finzi *et al.*,
96 2007; Iversen *et al.*, 2012). Specific site conditions (young, fast growing forests established on
97 abandoned soils previously used for agriculture or grazing) and the artificial nature of these
98 experiments (step-increase in [CO_2]) limit the direct application of the measurements to estimate the
99 N constraint on future global net primary production (*NPP*) and land C uptake. Nonetheless, the
100 fact that the *NPP* enhancement resulting from experimentally elevated CO_2 at several temperate
101 forest FACE experiments converged towards a common response size (Norby *et al.*, 2005) has led
102 modellers to attempt benchmarking exercises, to evaluate the capacity of terrestrial ecosystem
103 models to simulate average multi-year effects of CO_2 fertilisation (Sitch *et al.*, 2008; Piao *et al.*,
104 2013). But this consistency of response to CO_2 seen during the initial years has not been maintained
105 as the length of the experiments increased, showing that a single number does not capture the
106 complexities of ecosystem responses to eCO_2 : for instance, the *NPP* response strongly declined at

107 ORNL FACE towards the end of the experiment, while the Duke FACE site showed a sustained
108 eCO₂ response (Norby *et al.*, 2010; McCarthy *et al.*, 2010).

109 In this paper, we used 11 ecosystem models to investigate the effects of N availability on the eCO₂
110 response of forest productivity and C storage at two forest sites with fairly similar, temperate
111 climate (Köppen Cfa), comparable levels of N deposition, but contrasting vegetation: the evergreen,
112 needle-leaved Duke Forest (McCarthy *et al.*, 2010) and the deciduous, broad-leaved Oak Ridge
113 National Laboratory (ORNL) Forest (Norby *et al.*, 2010) FACE experiments. Since observed
114 ambient forest productivity and nitrogen requirement at the beginning of the experiment were
115 comparable at the two sites (see Results), our hypothesis was that the ecosystem models should be
116 able to explain the diverging long-term trends based on the different processes and time-scales
117 associated with the different vegetation types.

118 Our study forms part of a model intercomparison (A.P. Walker *et al.*, unpublished) looking at the
119 effect of eCO₂ on water (De Kauwe *et al.*, 2013), carbon (M.G. De Kauwe *et al.*, unpublished) and
120 nitrogen cycling. Each of the participating models incorporates the major processes by which the N
121 cycle affects the ecosystem's response to eCO₂ such as plant N uptake, net N mineralisation, and
122 the ecosystem N balance, as well as emergent ecosystem properties such as the nitrogen-use
123 efficiency of plant production (Fig. 1). The representation of these processes varies greatly among
124 models (Table A1), illustrating a lack of consensus on the nature of the mechanisms driving these
125 processes. Our objectives in this study were to:

- 126 i) understand the eCO₂ responses predicted by each model for the two sites in terms of their
127 assumptions and representations of C-N cycle processes, and
- 128 ii) use experimental observations to constrain these model projections, where possible identifying
129 the mechanisms that are supported versus those not.

130 Given the number and complexity of the C-N processes that determine the observed eCO₂
131 responses (Fig. 1), and the impracticality to measure every relevant C and N fluxes (e.g. N losses to
132 leaching and gaseous emission) and stocks (e.g. changes in organic soil N) with sufficient accuracy,
133 we aimed to identify those process representations that lead to responses qualitatively in agreement
134 with the available C and N cycle observations, rather than identifying the model best fitting the
135 observed NPP responses.

136

137 **2. Methods**

138 **2.1 Experimental sites**

139 The Duke Forest FACE site was located in a loblolly pine (*Pinus taeda* L.) plantation (35.97 °N,
140 79.08 °W) established in 1983 in an open woodland partially covered with grass harvested as fodder
141 (McCarthy *et al.*, 2007). The soil is relatively nutrient-poor, with forest production showing a
142 substantial response to N fertilisation (Oren *et al.*, 2001; Crous *et al.*, 2008; Maier *et al.*, 2008), as
143 evidenced from separate N fertiliser experiments in subplots, which were not analysed in the
144 present study. At the start of the Duke FACE experiment in August 1996, trees were 15 years old
145 and approximately 14-m tall, with a mean summer LAI of 3–4 m² m⁻² (for the dominant pine
146 species). The experiment consisted of three sets of paired plots (pairs of ambient and elevated
147 [CO₂], each 30 m in diameter) with different levels of tree productivities related to natural
148 variations in soil N availability, affecting ambient NPP, leaf area index (LAI), and the C allocation
149 to above- versus belowground compartments (Finzi *et al.*, 2002; Palmroth *et al.*, 2006; McCarthy *et al.*,
150 2007). One of each set of plots received continuous enhanced [CO₂] tracking ambient
151 conditions +200 μmol mol⁻¹.

152 The ORNL FACE site was located in a sweetgum (*Liquidambar styraciflua* L.) plantation (35.9 °N,
153 84.33 °W) established in 1988 on a grassland. The soil at the site had a silty clay-loam texture, and
154 was moderately well-drained and slightly acid (Norby *et al.*, 2001; Warren *et al.*, 2011). At the start
155 of the experiment, the approximately 90 trees per 25-m treatment plot were about 12 m tall and in a
156 linear growth phase. The LAI was 5.5 m² m⁻², and the canopy was no longer expanding (Norby *et al.*,
157 2002). Five treatments plots were established at the site, in two of which exposure to eCO₂
158 commenced in April 1998, and continued during daylight hours of each growing season (April-
159 November). The average daytime [CO₂] from 1998 to 2008 growing seasons was 547 μmol mol⁻¹ in
160 the two CO₂-enriched plots and 395 μmol mol⁻¹ in the three ambient plots.

161 2.2 Evaluation framework

162 Our approach to analysing the N-cycle dependence of the *NPP* response to eCO₂ was to break *NPP*
163 down into its component processes, thus benefitting from the suite of supplementary observations
164 on these processes provided at each experiment. We investigated how each model represented these
165 individual processes (Table A1) and compared model outputs against relevant observations. The
166 key C-N cycle processes controlling the ecosystem response to eCO₂ (Fig. 1) can be grouped into
167 two major categories: (a) Processes affecting nitrogen-use efficiency (*NUE*, see below), which has
168 both photosynthetic and whole-plant components, and (b) processes affecting N uptake (*fN_{up}*),
169 which include the rate of net N mineralisation (*fN_{min}*), the competitive strength of plant versus soil
170 microorganisms for N assimilation, and the ecosystem's balance of N inputs and losses (net
171 ecosystem N exchange; *NNE*). All variables used in the following are listed in Table A2.

172 2.1.1 Nitrogen-use Efficiency

173 The change of the gross primary production (GPP) with eCO_2 can be decomposed into the changed
 174 carbon return per unit of nitrogen investment into foliage, expressed as GPP per unit leaf N (N-
 175 based GPP ; GPP_N) and the change in the amount of leaf N. As the models only reported canopy-
 176 integrated values of GPP and foliar N (N_{can}), and GPP and autotrophic respiration (R_a) could not be
 177 measured directly, we analysed the eCO_2 effect on the relationship between NPP and N_{can} at the
 178 whole-ecosystem level, by analysing the N-based NPP (NPP_N) as:

$$179 \quad NPP_N = \frac{NPP}{N_{can}} = CUE \cdot GPP_N = \frac{NPP}{GPP} \frac{GPP}{N_{can}} \quad (1)$$

180 where CUE is the whole-plant carbon-use efficiency.

181 NPP is related to the amount of N available for growth by the N requirements set by the relative
 182 proportion of biomass growth of the different plant components and their C:N stoichiometry. We
 183 decomposed the whole-plant NUE into changes in tissue stoichiometry, changes in tissue allocation,
 184 and retranslocation as follows:

$$185 \quad NUE = \frac{NPP}{fN_{up}} = \frac{NPP}{(a_f \cdot n_f + a_r \cdot n_r + a_w \cdot n_w) \cdot NPP - f_{trans} \cdot n_f^{y-1} \cdot B_f} \quad (2)$$

186 where a are the fractions of NPP allocated to foliage (f), fine roots (r), and woody (w) biomass, n
 187 the respective tissue N concentrations, and $f_{trans} \cdot n_f^{y-1} \cdot B_f$ is the amount of N resorbed from the canopy
 188 in the previous year. Each of these terms is available from observations, including the amount of N
 189 retranslocated, which is calculated from the difference in N concentration between green foliage
 190 and leaf litter. Observed fN_{up} at ORNL FACE also included an estimate of foliar N uptake from
 191 atmospheric N deposition, a process not included in the models, at the rate of $0.6 \text{ g N m}^{-2} \text{ yr}^{-1}$ for
 192 both ambient and elevated plots (Norby & Iversen, 2006).

193 Net changes in vegetation C:N may differ from changes in NUE because N becomes allocated to
 194 tissues with different life-times. The effect of such changes is reflected in changes of the mean
 195 residence time of N in vegetation

$$196 \quad \tau_{Nveg} = \frac{N_{veg}}{fN_{up}} \quad (3)$$

197 where N_{veg} is the total N in vegetation.

198 2.2.2. Plant N uptake

199 The plant N uptake (fN_{up}) can be expressed as the sum of three factors: the rate of net N
 200 mineralisation into the inorganic N pool from litter and soil organic matter (SOM) decomposition
 201 (fN_{min}), the depletion of the soil inorganic N pool (ΔN_{inorg}); and any changes in the net ecosystem N
 202 exchange (NNE).

$$203 \quad fN_{up} = fN_{min} + NNE - \Delta N_{inorg} \quad (4a)$$

204 Changes in NNE depend on inputs from biological fixation (fN_{fix}) and atmospheric deposition (fN_{dep})
 205 and losses due to leaching (fN_{leach}) and gaseous emission (fN_{gas}), respectively:

$$206 \quad NNE = fN_{fix} + fN_{dep} - (fN_{leach} + fN_{gas}) \quad (4b)$$

207 The rate of net N mineralisation (fN_{min}) can also be separated into two factors: the effect of
 208 accumulating soil N during the course of the experiment and changes in the ratio of microbial N
 209 immobilisation to gross N mineralisation as follows:

$$210 \quad fN_{min} = \frac{N_{SOM}}{\tau_{N_{SOM}}} \quad (4c)$$

211 where N_{SOM} the size of the decomposing SOM pool, here including the litter layer, and $\tau_{N_{SOM}}$ its
 212 apparent turnover time. $\tau_{N_{SOM}}$ is constant, as long as the ratio of gross N mineralisation to
 213 immobilisation and the allocation of N to SOM pools with different life-times do not change.

214 Increasing immobilisation due to reduced litter quality will increase $\tau_{N_{SOM}}$, while increased gross
 215 mineralisation from increased microbial N uptake and release will decrease $\tau_{N_{SOM}}$. Insufficient
 216 observations were available to constrain the change of fN_{up} component processes during the course
 217 of the experiment (Iversen *et al.*, 2011).

218 2.2.3 Ecosystem stoichiometry

219 The total ecosystem C stored in a forest relates to the total ecosystem N as follows (Rastetter *et al.*,
 220 1992):

$$221 \quad C_{org} = \left(f_{veg} \frac{C_{veg}}{N_{veg}} + (1 - f_{veg}) \frac{C_{soil}}{N_{soil}} \right) N_{org} \quad (6)$$

222 where N and C are the nitrogen and carbon pool, respectively, for vegetation (veg), soil ($soil$) or
 223 total organic (org), and f_{veg} is the fraction of ecosystem N in vegetation. For the sake of simplicity,
 224 litter pools were subsumed to the soil pools.

225 2.3 Observations

226 Observed annual changes in C and N cycle parameters were taken from the FACE Data
227 Management System web-repository (<http://public.ornl.gov/face>), as well as published literature,
228 where indicated below. Nitrogen cycle observations from Duke FACE were only available from
229 1996 to 2005, so most of the analyses in this paper are focussed on this period, although NPP and
230 meteorological forcing data for each treatment plot were available until 2007. The ORNL FACE
231 experiment ran from 1998 to 2009, and data through 2008 were available for this study.

232 For Duke FACE, standing biomass and biomass production in each plot for three plant
233 compartments (foliage, fine roots, and woody biomass, including branches and coarse roots) were
234 taken from McCarthy *et al.* (2010), using the C and N concentration data for each plant
235 compartment reported by Finzi *et al.* (2007) to estimate C and N stocks and fluxes. Plant N
236 requirements and uptake were calculated from these data following Finzi *et al.* (2007). Forest floor
237 and soil organic matter C and N concentrations were obtained from Lichter *et al.* (2008).

238 For ORNL FACE, standing biomass, annual biomass production, their respective C and N
239 concentrations, as well as inferred N requirements and plant N uptake by plot and plant
240 compartment (foliage, fine roots and woody biomass, including branches and coarse roots) were
241 obtained from (Norby *et al.*, 2010). Initial and final soil organic matter stocks and their C and N
242 concentrations were obtained from Johnson *et al.* (2004), Jastrow *et al.* (2005) and Iversen *et al.*
243 (2012). Differences in sampling design and soil bulk density measurements prevent accurate
244 calculation of the change in soil C and N during the course of the experiment (Iversen *et al.*, 2012).
245 Comparing the % C and N data in Johnson *et al.* (2004) and Iversen *et al.* (2012), we estimated that
246 $10 \pm 21\%$ of the greater C and N stocks in the elevated plots at the end of the experiment (Iversen *et al.*
247 *et al.*, 2012) were due to eCO₂, while the rest were due to initial differences among the plots.
248 Combined with the standard errors of the measurements, eCO₂ led to an increase in SOM to a depth
249 of 90-cm of $160 \pm 188 \text{ g C m}^{-2}$, and $11.6 \pm 24.6 \text{ g N m}^{-2}$ between the beginning and end of the
250 experiment.

251 The data analyses outlined in Section 2.2 were made using data by plot and year. For Duke FACE,
252 responses were calculated per plot-pair, and reported as mean and standard error across the three
253 pairs. For ORNL FACE, the analyses were done with the mean and standard error across the
254 average of the two eCO₂ plots compared to the average of the three ambient CO₂ plots.

255 **2.4 Ecosystem models**

256 In this study, we used on the same set of 11 process-based ecosystem models described by A.P.
257 Walker *et al.* (unpublished), encompassing stand (GDAY, DAYCENT, TECO), age/size-gap

258 (ED2.1), land surface (CABLE, CLM4, EALCO, ISAM, O-CN), and dynamic global vegetation
259 (LPJ-GUESS, SDGVM) models. A detailed account of the major N cycle processes represented in
260 each model is given in Table A1. The model simulations covered the time periods representative of
261 the FACE experiments. Meteorological and [CO₂] data, as well as site history and stand
262 characteristics, were provided in a standardised manner (<http://public.ornl.gov/face>).

263 All models (except CABLE and ED2.1) followed a similar protocol to derive the initial soil C and
264 N pools of the sites, which considered the past land-use, as well as the historic evolution of
265 atmospheric CO₂ concentration and N deposition, while site-specific meteorological driver data
266 from during the FACE experiments were used throughout the spin-up. The forest vegetation of the
267 plots was initialised such that the forests had the correct age and structure, as far as considered by
268 the model, at the beginning of the eCO₂ treatment. Details of the spin-up phase varied among
269 models because of differences in model structure (A.P. Walker *et al.*, unpublished). Inherently
270 different assumptions of the models regarding soil C residence times and ecosystem N loss rates, as
271 well as pre-FACE grassland productivity and N fixation, led to a notable spread in the initial
272 amounts of modelled C and N pools, net N mineralisation rates and thus NPP despite the common
273 initialisation protocol.

274 Model outputs were provided at hourly or daily time steps, as appropriate. These outputs contained
275 estimates of the various C, N, and water fluxes and pools.

276

277 3. Results

278 3.1 Overall response to eCO₂

279 Observed ambient *NPP* and inferred fN_{up} at Duke FACE were both slightly larger than at ORNL
280 FACE (Fig. 2-3a,b), implying that the whole-plant *NUE* was similar between the sites (Fig. 4) at
281 121 ± 2 gC g⁻¹N in the ambient plots (1997-2005 mean) for Duke FACE and 129 ± 13 gC g⁻¹N at
282 ORNL. This similarity between sites is in contrast to an earlier study (Finzi *et al.*, 2007) because the
283 corrections in biomass estimates by McCarthy *et al.* (2010) resulted in an downward adjustment in
284 the estimate of *NUE* at Duke Forest.

285 The interquartile range of the model ensemble included the observed ambient *NPP* at both sites. But
286 there was significant spread across the models, resulting to a large extent from different model spin-
287 ups, which led to different levels of N constraints on plant production. Only a few of the models
288 (GDAY, O-CN) captured the decline of *NPP* in the ORNL ambient plots related to declining soil N
289 availability over the course of the experiment (Norby *et al.*, 2010; Garten *et al.*, 2011). While the
290 models on average matched the inferred, observation-based fN_{up} at Duke Forest, they overestimated

291 the fN_{up} at ORNL (Fig. 3). On average, the models slightly underestimated NUE at Duke and more
292 strongly at ORNL FACE (Fig. 4). The primary cause for the underestimation was a high-bias in the
293 simulation of the fractional (C) allocation to fine roots at both sites (M.G. De Kauwe *et al.*,
294 unpublished.). At ORNL FACE, this difference was accentuated by higher modelled than observed
295 N concentration of the fine roots (average 1.4% modelled versus 0.7% observed).

296 Elevated CO_2 increased NPP in the initial (first) year of the experiments by $25\pm 9\%$ and $25\pm 1\%$ at
297 Duke and ORNL FACE, respectively; according to the measurements (Fig 2c,d and Fig. 5a,b). Most
298 models simulated an initial (first year) increase of NPP due to eCO_2 that was close to the
299 observations. Notable exceptions were CABLE and CLM4, which systematically underestimated
300 the initial response at both sites, as well as EALCO and ISAM, which overestimated the response
301 for Duke FACE (Fig. 5a,b). Nonetheless, no model simulated the underlying changes in fN_{up} and
302 NUE correctly for both sites. At Duke Forest, according to the measurements, the increase in NPP
303 was associated with a strong increase in fN_{up} . The models generally underestimated the observed
304 increase in fN_{up} and overestimated the increase in NUE . At ORNL, according to the measurements,
305 the initial increase in NPP was associated with nearly equal increases of fN_{up} and NUE (Fig. 5).
306 Some models simulated a change in NUE in agreement with the observations (DAYCENT, GDAY,
307 ISAM, LPJ-GUESS, O-CN, TECO), but most models had a tendency to underestimate the increase
308 in fN_{up} .

309 The observed responses at the end of the experiment differed strongly between the two experiments
310 (Fig. 5c,d): the CO_2 -response of NPP at Duke forest was maintained throughout the experiment,
311 because the initial increase in fN_{up} was sustained with little change in whole-plant NUE . At ORNL,
312 the CO_2 -response of NPP declined over time, because the initial increase in NUE declined due to
313 higher allocation to N-rich fine roots. At the end of the experiment, NUE and fN_{up} were similar
314 between ambient and elevated plots.

315 Most models showed signs of PNL (i.e. a progressively smaller enhancement of NPP due to N
316 limitation) towards the end of the experiment at both sites (Fig. 5c,d), but with varying strength and
317 timing, causing an increasing spread among the models with duration of the experiment. At Duke
318 FACE, the models largely failed to capture the sustained NPP response to 11 years of eCO_2 . The
319 decline occurred despite increasing whole-plant NUE , because the models were not able to maintain
320 an increased fN_{up} as observed (with the exception of ED2.1). At ORNL FACE, three out of the 11
321 models correctly simulated the 10% decline of the initial response towards the end of the
322 experiment (DAYCENT, LPJ-GUESS, SDGVM), and two models (GDAY, O-CN) showed an even
323 stronger decline, related to an early simulated onset of N-limitation in the ambient treatment. Two
324 models (ED2.1 and TECO) predicted an increase in the NPP response over time, fuelled by

325 increases in plant N uptake, which were supported by a large pool of easily degradable SOM and
326 inorganic N prescribed as initial conditions. Contrary to the observations, NUE and vegetation C:N
327 strongly increased at ORNL in most models by the end of the experiment.

328 3.2 Processes affecting nitrogen-use efficiency

329 3.2.1 N-based GPP and NPP

330 Models differed strongly in their initial NPP_N response to eCO_2 (Fig. 6), generally overestimating
331 the observed initial $11\pm 8\%$ increase in the NPP_N at Duke FACE and underestimating the observed
332 $35\pm 4\%$ increase at ORNL FACE. Although N limitation did not strongly affect GPP_N in the first
333 year in most models, there was substantial difference in the first year's response among the models,
334 in particular at ORNL FACE. Two models (CABLE and CLM4) showed an exceptionally low
335 initial response of NPP at both sites (Fig. 5). This low response was related to a near-zero response
336 of the GPP_N (Fig. 6a,b). In CLM4, this response resulted from the assumption that plants down-
337 regulate GPP directly when N-limited: CO_2 fertilisation of GPP is calculated in the absence of N
338 limitation, and then reduced using N-limitation scalars if fN_{up} is insufficient to support this amount
339 of productivity. This low response did not happen in other models that follow a similar approach
340 (DAYCENT and ED2.1), because of sufficient initial N supply. Another class of models simulated
341 photosynthesis based on foliar N content (CABLE, GDAY, LPJ-GUESS, O-CN, SDGVM, TECO).
342 In these models, N-limitation on GPP acts via foliar N concentrations: limited N availability
343 reduces foliage N, which feeds back to limit GPP . This limitation takes time to develop, such that it
344 was absent or weak in the initial response, but a strong component of down-regulation in the longer
345 term (Fig. 6c,d).

346 Model predictions of the eCO_2 effect on the other component of NPP_N , carbon-use efficiency
347 (CUE , eqn. 1) can be readily categorised into three groups as follows: (i) models that assume that
348 NPP is a fixed proportion of GPP (GDAY and DAYCENT) showed no change in CUE ; (ii) models
349 that estimate R_a directly from biomass and temperature (CABLE, CLM4, EALCO, ED2.1, ISAM,
350 LPJ-GUESS, SDGVM, O-CN and TECO) predicted a transient increase in CUE , because the
351 increase in respiration due to increased biomass lagged behind the immediate eCO_2 effect on GPP .
352 These models generally showed that CUE returned to its original value within the time course of the
353 experiment (10 years). In addition to these processes, (iii) some models (CABLE, O-CN) increased
354 R_a under nutrient stress, when stoichiometric constraints prevented allocation of the assimilated C
355 to growth. For example, at ORNL FACE the CUE in O-CN fell noticeably during the last years of
356 the experiment (Fig. 6d). This change was driven by a growing N-limitation, which resulted in a
357 build-up of labile C. Increased respiration was used as a mechanism to remove this excess
358 accumulated C.

359 3.2.2 Whole-plant NUE

360 With eCO₂, observed *NUE* at Duke Forest increased by 5±2%, mainly because of a shift of
361 allocation towards lower C:N tissue (wood), while the 4±3% decline in foliar N had little effect on
362 *NUE* (Fig. 7). Despite the initially observed increase in *NUE* at ORNL FACE, *NUE* did not change
363 over the course of the experiment (+2±5%), as the effects of increased tissue C:N were
364 compensated by increased allocation towards N-rich roots.

365 In the observations, the fraction of foliar N retranslocated before leaf-shedding did not change
366 significantly with eCO₂ (-1.1±0.4% at Duke Forest, 0.0±14.3% at ORNL FACE), such that the
367 retranslocation flux scaled with changes in total canopy N (see Fig. 6). In most models (except
368 EALCO), the retranslocation fraction did not vary with foliar N (or root N) content (Table A1),
369 such that, in agreement with observations, the retranslocation flux scaled with the total foliage (and
370 root) N change. The effect of eCO₂ on *NUE* can therefore be simply separated into its effects on
371 stoichiometry and allocation (Fig. 7) for those models that produced all of the variables required to
372 do these calculations. The model ensemble includes four alternative hypothesis combinations as to
373 how whole-plant *NUE* changes with eCO₂, namely

- 374 (i) assuming allocation and tissue stoichiometry to be constant (CLM4, TECO);
- 375 (ii) assuming flexible C:N ratios, but N-insensitive partitioning fractions (CABLE, GDAY,
376 EALCO, SDGVM);
- 377 (iii) assuming constant tissue C:N ratios, but increasing root allocation with N stress (ED2.1); and
- 378 (iv) assuming the stoichiometry to be flexible and root allocation to increase with N stress
379 (DAYCENT, ISAM, LPJ-GUESS, O-CN).

380 While the modelled *NUE* responses differed in magnitude among models, each model individually
381 simulated similar trends at both sites, such that none of the models was able to simulate the
382 observed difference in the *NUE* response between the sites, in particular the observation-based
383 interannual variability of the response at ORNL (Fig 4. and 5). CABLE, which allows for
384 acclimation of tissue C:N only within narrow bounds, showed hardly any change in *NUE*; similar to
385 CLM4, which simulates fixed tissue stoichiometry and allocation fractions (Fig. 7). In contrast,
386 models with a large flexibility in tissue stoichiometry (GDAY, LPJ-GUESS, O-CN) consistently
387 showed a stronger change of *NUE* due to increases in tissue C:N ratios than due to changes in
388 allocation at both sites. The flexible C:N models showed a strong decline of foliar N at both sites,
389 leading to a larger than observed decline in some models (Duke: CABLE, GDAY, LPJ-GUESS, O-
390 CN; ORNL: GDAY), which contributed to these models' excessive *NUE* response to eCO₂.

391 The combined effect of the changes in allocation and stoichiometry in most models was that τ_{Nveg}
392 first declined, as a result of larger growth of fast-overturning tissues (i.e. increased foliar growth as
393 a result of increased *NPP*), but increased later in the experiment as tissue N concentration dropped
394 and more N became incorporated into woody tissue. This model outcome is consistent with the
395 observed response at Duke, but not ORNL FACE, where the strong increase of fine-root growth
396 resulted in a stronger decline of τ_{Nveg} than suggested by the models.

397 In summary, models that include representations of flexible tissue stoichiometry, photosynthesis-
398 calculation based on prognostic foliar N, and increasing fine root allocation under nutrient stress
399 were generally more consistent with observed trends of the component processes. However,
400 because of difficulties in capturing the timing and magnitude of the response of stoichiometry and
401 allocation (as well as diverging predictions of plant N uptake; see Section 3.3), these models did not
402 appear to be generally superior to the other models considered here in terms of predicting the CO₂
403 response of *NPP*.

404 3.3 Processes affecting plant N uptake

405 As outlined in the methods (eqn. 4), changes in modelled fN_{up} can be attributed (a) changes in the
406 rate of net N mineralisation (fN_{min}), which depends on the total amount of soil organic matter N
407 (N_{SOM}) and its turnover time (τ_{NSOM}); (b) changes in the rate of depletion of the soil inorganic
408 matter pool (ΔN_{inorg}); and (c) changes in the net ecosystem N exchange (*NNE*).

409 In SDGVM, fN_{up} was driven with observations and therefore this model is not further considered in
410 this section. Among the other models, there are two alternative implementations of the processes
411 that allow for a preferential increase of fN_{up} compared to microbial N immobilisation under eCO₂,
412 leading to contrasting predictions (Fig. 8a,b).

413 The first, employed by CLM4, is to increase the relative competitiveness of plants versus microbes
414 for N. The plant's N demand is a function of potential *GPP*, which increases with eCO₂.

415 Conversely, the microbial N demand does not change strongly with eCO₂, because CLM4 assumes
416 fixed tissue C:N and therefore simulates no change in litter quality with eCO₂, which would
417 increase the N requirement of microbes and therefore immobilisation. As a result, CLM4 showed a
418 sustained increase of fN_{up} at ORNL, because less N was immobilised than under ambient conditions
419 (Fig. 8c).

420 The second mechanism is an emergent property of the CENTURY model (used by CABLE,
421 DAYCENT, GDAY, LPJ-GUESS and O-CN): initial increases in fN_{up} due to enhanced *NPP* lowers
422 soil inorganic N availability, which increases the C:N of the newly formed SOM according to an
423 empirical relationship. This reduces N immobilisation during litter decomposition, as less N needs

424 to be sequestered for the same amount of litter C transfer, increasing the availability of inorganic N
425 for fN_{up} (Fig. 8e). In most of these models, the increase was dampened or reversed within a few
426 months or years because the models also apply a flexible tissue C:N. Increased N stress increased
427 tissue (and therefore also litter) C:N ratios, leading to higher microbial N immobilisation and
428 therefore a reduction of the net N mineralisation (fN_{min}) to ambient or even below-ambient rates,
429 reflected as an increase in τ_{NSOM} , and therefore a decrease in the availability of inorganic N (Fig.
430 8d).

431 A second factor affecting the eCO_2 response of fN_{up} is the initial size of the inorganic N pool. Some
432 models simulated an initial excess of inorganic N relative to plant N demand due to the site history
433 (or the spin-up procedure; ED2.1, CABLE at Duke FACE and TECO at ORNL). An example is
434 CABLE at Duke Forest (Fig. 8e), in which the initial increase of fN_{up} was supported by the initially
435 available inorganic N pool. This pool became exhausted after few years of the experiment, leading
436 to lower fN_{up} relative to the ambient plots in the later years of the experiment. The TECO model at
437 ORNL had a much larger SOM pool, and with it gross N mineralisation, than required by the
438 forest's productivity, leading to a constant excess supply of N, which supported fN_{up} under eCO_2 .

439 The third factor is the ecosystem N balance (NNE), which depends on rates of input via deposition
440 and fixation, and rates of loss via leaching and volatilisation. A few models in the ensemble
441 (CABLE, CLM4) simulated biological N fixation explicitly, but none of them suggested that eCO_2
442 would alter fixation such that it would affect the net N balance. For the other models, the principal
443 difference affecting total ecosystem N balance was whether the N losses were assumed to be
444 proportional to the amount of N mineralised (CABLE, CLM4, GDAY, TECO) or whether they
445 were a function of the simulated inorganic N concentration (CABLE, CLM4, EALCO, ISAM, LPJ-
446 GUESS, O-CN). In some of the models (CABLE, CLM4, DAYCENT, GDAY, LPJ-GUESS, O-
447 CN), ecosystem N losses were reduced, but the causal mechanism differed between the models: for
448 example GDAY, in which fN_{up} is assumed to be independent of plant N demand, and therefore
449 eCO_2 , fN_{min} declined as a consequence of the higher microbial immobilisation (higher litter C:N),
450 which directly decreased the gaseous N losses in addition to reducing N leaching because of lower
451 soil inorganic N. In O-CN, higher fN_{up} and increased N immobilisation led to lower inorganic N,
452 causing both lower gaseous and leaching losses.

453 In most models, the change in NNE was of the order of 1 g N m^{-2} over 10 years. This reduction in N
454 loss was not sufficient to prevent the onset of progressive N limitation, in forests that take up
455 $8.3 \pm 0.4 \text{ g N m}^{-2} \text{ yr}^{-1}$, on average. The only exception to this pattern was the simulation of CLM4 at
456 Duke FACE, where larger increases in fN_{up} substantially reduced gaseous N losses during autumn
457 and winter, leading to a cumulative increase in fN_{up} of 12 g N m^{-2} (Fig. 8a). While this sustained

458 increase avoided the progressive decline of fN_{up} in CLM4, it was not sufficient to explain the
459 observed increase in vegetation N at Duke FACE.

460 3.4 Time-integrated effect of eCO₂ on ecosystem C and N

461 At Duke, about 80% of the observed increase in cumulated NPP ($3.1 \pm 0.6 \text{ kg C m}^{-2}$; 1997 to 2005)
462 was sequestered in vegetation ($2.5 \pm 0.5 \text{ kg C m}^{-2}$) and forest floor C ($0.3 \pm 0.1 \text{ kg C m}^{-2}$), while soil C
463 declined by about $0.2 \pm 0.1 \text{ kg C m}^{-2}$ (Fig. S1). These changes were associated with increased
464 vegetation N ($12.2 \pm 2.9 \text{ g N m}^{-2}$), litter N ($6.8 \pm 2.6 \text{ g N m}^{-2}$) and decreased soil N ($25.0 \pm 7.0 \text{ g N m}^{-2}$).
465 At ORNL, the observed enhancement of NPP ($1.7 \pm 0.4 \text{ kg C m}^{-2}$; 1998-2008) did not result in a
466 significant change of biomass ($0.0 \pm 0.7 \text{ kg C m}^{-2}$ and $1.2 \pm 1.7 \text{ gN m}^{-2}$, respectively), but soil C and
467 N pools were slightly increased ($0.2 \pm 0.2 \text{ kg C m}^{-2}$, and $11.5 \pm 12.3 \text{ g N m}^{-2}$, respectively).

468 Most of the models suggested that a large fraction of the NPP enhancement remained in vegetation
469 C (Fig. S1), in agreement with the observed trends at Duke FACE, but in disagreement with those
470 observed at ORNL FACE. Nevertheless, most models underestimated vegetation C sequestration at
471 Duke FACE, because they underestimated the NPP enhancement and failed to predict the decline in
472 SOM. Most models overestimated vegetation C sequestration in ORNL FACE, mostly related to
473 failure in capturing accurately the allocation pattern and response (M.G. De Kauwe *et al.*,
474 unpublished.; Fig. S1).

475 The large observed increase of vegetation biomass at Duke Forest was supported mostly by a
476 redistribution of N from soil to the vegetation, as soil N stocks in the upper soil layers have likely
477 declined over the course of the experiment (Fig. 9a). However, there were significant differences in
478 the magnitude of the transfer and vegetation C:N changes among the plots, causing large
479 uncertainty in the attribution of the observed vegetation C increase. Although fN_{up} also increased in
480 ORNL FACE, there was not a sustained increase in biomass N and C because of rapid turnover of
481 leaves and roots did not lead to a sustained increase in biomass N and C, which instead caused C
482 and N sequestration in SOM (within the detection limit; Fig. 9b). At both sites, bulk vegetation C:N
483 slightly decreased with eCO₂, despite the larger C:N in foliage, due to the larger contribution of
484 foliage and root biomass to total biomass.

485 Consistent with the observations, increased organic ecosystem N (N_{org}) played a minor role in most
486 models (Fig. 9). The exception of ED2.1 and TECO at Duke Forest was related to the assumed
487 initial conditions (Section 3.3). Changes in the ecosystem N balance, i.e. reduction of N losses, led
488 to less than 500 g C m^{-2} additional C sequestration (CLM4 and CABLE at Duke Forest; DAYC and
489 LPJ-GUESS at ORNL FACE). Contrary to the observations, models that assume a flexible tissue
490 C:N ratio (CABLE, EALCO, GDAY, LPJ-GUESS, O-CN) predicted that a large fraction of the
491 increase in ecosystem C storage at both sites due to eCO₂ resulted from the increase of vegetation

492 C:N ratios (Section 3.2). Only CLM4, which assumes fixed tissue stoichiometry, correctly predicted
493 the decline in total vegetation C:N ratio at Duke Forest and the ensuing reduction in vegetation C
494 storage capacity; this response resulted from the increase in foliar and root biomass. Changes in
495 litter and soil C:N were generally of lesser importance in absolute terms, and roughly agreed with
496 the observations. An exception to this was the projected large increase in litter C:N by LPJ-GUESS
497 at ORNL FACE associated with large litter fall of the deciduous trees and a strong decline in leaf N
498 concentrations.

499 At Duke Forest, most models suggested that there was a net transfer of N to the vegetation (as a
500 result of the increased fN_{up}), which supported C accumulation in vegetation. However, the predicted
501 increase was always less than half that observed. In LPJ-GUESS the cumulative effect was a net
502 transfer of N to the soil, probably related to the large fraction of C (and thus N) allocated to fast-
503 overturning tissues (M.G. De Kauwe *et al.*, unpublished.). A net N transfer to vegetation initially
504 also occurred in most models at ORNL FACE. However, in GDAY, LPJ-GUESS and O-CN the
505 larger litter fall and the declined litter C:N ratio at the deciduous site led to increased
506 immobilisation of N during decomposition. This provided a mechanism by which plant-available N
507 became trapped in the soil organic matter pool, effectively reducing the fraction of ecosystem N
508 stored in vegetation, consistent with the PNL hypothesis.

509

510 **4. Discussion**

511 The analyses presented here have separated the eCO₂ response into time-dependent, observable
512 components of the C and N cycle responses, which can be used to evaluate individual model
513 processes and identify key model weaknesses, as well as to identify the need for more observational
514 constraints. The climate and N inputs, as well as the initial, ambient, levels of production, N uptake
515 and nitrogen-use efficiency, were similar between the two sites, leading to the expectation that the
516 different long-term trends in the eCO₂ response of NPP and N uptake at Duke and ORNL FACE
517 could be explained by processes associated with the different vegetation types encoded in the
518 models. Despite the success of the model to simulate the initial eCO₂ response of NPP at both sites,
519 the models did not encode the relevant processes to explain the observed differences. Rather most
520 models followed the ORNL trajectory (progressively increasing N limitation) at both sites. In the
521 following, we discuss the process representation of the most important C-N cycle linkages that
522 contribute to the site and model-data differences.

523 **4.1 Model responses and underlying processes**

524 *Plant N uptake and net N mineralisation*

525 The increase in fN_{up} at Duke FACE was twice as large as that seen at ORNL FACE, in absolute
526 terms and when integrated over the time of the experiment. This is a key factor in the observed,
527 divergent *NPP* response at the two sites. The ensemble of models generally failed to simulate the
528 magnitude of the observed increase in fN_{up} and the large difference between the sites, although some
529 of the models possess mechanisms to increase root growth, and the specific N_{inorg} uptake capacity of
530 roots or whole plants, under N stress. In most models, fN_{up} was tightly constrained by fN_{min} , but
531 only few ecosystem-scale observations are available for this quantity (Iversen *et al.*, 2011). At
532 ORNL FACE, the increased fN_{up} was likely related to the presence of plant-available N below the
533 rooting zone of trees at the beginning of the experiment, resulting from past land-use. Increased tree
534 rooting depth and likely stimulation of SOM decomposition in these layers have added plant
535 accessible N (Iversen *et al.*, 2008; 2011). Consideration of SOM depth profiles is missing in most
536 ecosystem models, but this is likely to be relevant only under site conditions in which past land-use
537 determines the depth distribution of SOM. Increased microbial and fungal SOM decomposition
538 following increased rhizodeposition (so called ‘priming’) is probably the cause of the large N
539 transfer from soils to plants at Duke FACE (Drake *et al.*, 2011); this is a further process not
540 represented by the model ensemble. It is an open question whether this finding implies that models
541 that do not incorporate such a mechanism must also have a low *NPP* response to gradually
542 increasing atmospheric $[CO_2]$. Under these conditions, the more gradual increase in plant N-
543 demand (Luo & Reynolds, 1999) might be satisfied by other mechanisms such as the tightening of
544 the ecosystem N balance or increased N fixation. Moreover, CENTURY-based models
545 (DAYCENT, GDAY, OCN, LPJ-GUESS, TECO), which mimic the net transfer of N from soils to
546 vegetation under increasing N stress, showed that the net N transfer based on N mining was limited.
547 The pool of easily degradable N-rich material declined as a result of the increased N mining and
548 declining litter quality, suggesting that ‘priming’ might be a temporary process relieving N stress.

549 *NUE and ecosystem stoichiometry*

550 The observed initial increase in whole-plant *NUE* that was stronger at ORNL than at Duke Forest,
551 which can be largely explained by the different magnitude of decline in foliar N concentrations and
552 the diverging trends of total canopy N (Fig. 6). The *NUE* enhancement decayed at ORNL FACE
553 with increasing root allocation during the experiment, such that was no strong change of *NUE* with
554 eCO_2 at both sites. Including flexible C:N stoichiometry, alongside increased below-ground
555 allocation in response to eCO_2 and increased plant N-demand (M.G. De Kauwe *et al.*,
556 unpublished.), appeared to be an important feature allowing the *NUE* response to CO_2 to be
557 captured because of the significant changes in foliar N concentrations. However, models that
558 simulate flexible stoichiometry tended to overestimate the whole-plant *NUE* increase with eCO_2 .

559 The likely reason for this overestimation is that the predicted changes in tissue C:N are not based on
560 a hypothesis-driven prediction of C:N changes, but rather the emergent model outcome, as flexible
561 stoichiometry in these models is the means to regulate C assimilation given plant available N.
562 While the marginal change in photosynthetic capacity can be larger than the marginal change in
563 foliar N (Friend *et al.*, 1997), this does not seem to be sufficient to keep tissue C:N within observed
564 bounds, as shown by an exaggerated decline in foliar N concentrations at both sites. Other
565 regulatory mechanisms, such as the acclimation of *CUE* under N stress as implemented in the O-
566 CN model, can limit the reduction in tissue C:N ratios to variations within predefined bounds, but it
567 is unclear whether such a mechanism exists in reality. Modelling approaches that maximise leaf
568 photosynthetic gain given N and C availabilities may provide a more reliable framework to predict
569 stoichiometric flexibility (Medlyn, 1996a; McMurtrie *et al.*, 2008; Xu *et al.*, 2012; McMurtrie &
570 Dewar, 2013).

571 At both sites, the $e\text{CO}_2$ effect on NPP_N according to the measurements had initially increased (more
572 so at ORNL than Duke FACE) but then declined to very low values of enhancement. In deciduous
573 trees at both sites, this decline was not associated with a change in the relationship of
574 photosynthetic biochemistry (V_{cmax} : the maximum rate of carboxylation, and V_{jmax} , the maximum
575 rate of electron transport at saturating irradiance) with leaf N (Norby *et al.*, 2010; Ellsworth *et al.*,
576 2011), whereas at Duke Forest, older pine needles showed a reduced V_{cmax} per unit leaf N
577 (Ellsworth *et al.*, 2011). A number of models implement a leaf-N dependence of photosynthetic
578 biochemistry (Table A1), and a few of them captured the overall trend in foliar N and GPP_N .
579 However, there was a large spread in the simulated $e\text{CO}_2$ response of GPP_N both initially and in the
580 longer-term, despite the fact that (with the exception of DAYCENT) all models inherit the CO_2 -
581 sensitivity of photosynthesis from the Farquhar model (Farquhar *et al.*, 1980). Since the effect of
582 $e\text{CO}_2$ on GPP_N is immediate, the uncertainty in the modelled initial GPP_N response is independent
583 of the representation of N cycle feedbacks, and therefore not affected by the step-increase in CO_2 .
584 The differences among models were maintained when analysing daily data with a restricted range
585 of meteorological parameters, instead of annually integrated values: a finding which excludes any
586 difference due to phenological biases (A.P. Walker *et al.*, unpublished) that could also affect GPP_N .
587 The likely cause for these differences is alternative assumptions about the fraction of the canopy
588 that is limited by light availability versus carboxylation rate, related to the canopy scaling of N and
589 the depths of the canopy (Medlyn, 1996b). Varying stomatal responses to $e\text{CO}_2$ may also have
590 played a role (De Kauwe *et al.*, 2013). Reducing this uncertainty requires a better representation of
591 the changes of foliar N and the slope of the $V_{\text{jmax}}:V_{\text{cmax}}$ relationship within the canopy and across
592 different ecosystems (Maire *et al.*, 2012). At the ecosystem-level, alternative data sources, light-
593 response curves of net ecosystem exchange, or GPP , derived from eddy-covariance measurements,

594 could facilitate the evaluation of the canopy-level light response across ecosystem types (Lasslop *et al.*, 2010; Bonan *et al.*, 2012).
595

596 *Ecosystem N balance*

597 Uncertainties in the observed changes of soil N stocks prevent any statistically meaningful
598 assessment of whether eCO₂ increased N capital due to changes in N inputs or outputs. Some
599 models simulated increased plant N availability through reduced N losses from the ecosystem.
600 While these mechanisms added up to 12 g N m⁻² (accumulated over the length of the experiment) in
601 the most extreme case, they did not contribute strongly to the simulated C sequestration. Changes in
602 the N balance may be an important factor in modelled eCO₂ responses (Rastetter *et al.*, 1997), but
603 the effect was not very pronounced in the ensemble used in this study. None of these N-loss
604 reduction mechanisms was sufficient to explain the observations at Duke FACE. In agreement with
605 previous observationally based studies (Drake *et al.*, 2011), we conclude that a mechanism that
606 increases plant N availability under plant N stress based on enhanced mineralisation of organic N is
607 required for models to explain the observed trends at Duke.

608 **4.2 Limits of the observational constraints**

609 The process inferences above rely on uncertain observations and implicit assumptions that require
610 careful interpretation. The estimates of plant N uptake were inferred from the biomass production of
611 plant tissues, their N concentrations, and foliar N recovery upon leaf shedding. Estimates of *NPP*
612 and fN_{up} are therefore not independent, so the estimated whole-plant *NUE* should be considered
613 with caution. Increases in *NPP* without statistically significant changes in tissue N concentrations
614 imply an increase in fN_{up} , irrespective of whether the rhizospheric N uptake has indeed increased, or
615 whether changes in foliar N retention (or perhaps labile amino-acid reserves not accounted for in
616 the observed tissue N concentration changes) have affected the plants' N balance. This situation
617 leads to uncertainty in the fN_{up} estimates for an individual year, and therefore the eCO₂ response in
618 the initial year of the experiment. However, the error associated with unaccounted-for reserves
619 diminishes when the estimates are integrated over time, and on average, the translocation fractions
620 did not change with time in the observations, further reducing the longer-term error.

621 Uncertainty also results from the difficulties in measuring below-ground biomass and production,
622 which is a fairly small contribution to total *NPP* at Duke Forest, but up to 40% of total *NPP* at
623 ORNL under eCO₂ (Iversen, 2009; McCarthy *et al.*, 2010). Observations of fine-root biomass
624 should give suitably constrained estimates of the relative increase in root allocation under eCO₂.
625 But uncertainty in the absolute below-ground carbon flux, and specifically C flux to mycorrhizae,
626 propagates to uncertainty in annual *NPP* -- and thus in the inferred N requirements to sustain the
627 eCO₂ response.

628 There is also substantial uncertainty in the observation-based estimates of net SOM changes with
629 eCO₂, resulting from a small signal-to-noise ratio and uncertainties in the sampling and analyses of
630 the soil data (Jastrow *et al.*, 2005). This uncertainty is primarily due to the spatial variability of
631 SOM, particularly for N (Iversen *et al.*, 2012). The uncertainty in these measurements is large
632 enough to preclude reliable quantification of the net eCO₂ effect on total soil and ecosystem C and
633 N over the 10 years of the experiment (Fig. 9 and S1), as the expected change in SOM due to CO₂ is
634 rather small. Therefore, the observations from Duke and ORNL Forest do not provide a robust
635 constraint on the model N balance. Nonetheless, independent studies suggest that increased
636 microbial decomposition may have resulted in a net transfer of N to vegetation at Duke FACE
637 (Drake *et al.*, 2011; Hofmockel *et al.*, 2011; Drake *et al.*, 2013), whereas increases in microbial
638 activity with eCO₂ may have been insufficient to compensate for the increased accumulation of N in
639 soil organic matter at ORNL FACE (Iversen *et al.*, 2012).

640 Year-to year variations in meteorological parameters influence both the ambient C- and N cycling
641 at the sites and the response to eCO₂. These influence range from the direct effect of temperature on
642 the CO₂ sensitivity of photosynthesis (Hickler *et al.*, 2008), to indirect effects resulting from
643 interannual variations in levels of drought-stress (and thus eCO₂ - water-use efficiency interactions;
644 De Kauwe *et al.*, 2013) or nitrogen availability, following the sensitivity of soil organic matter
645 decomposition to soil temperature and moisture (Melillo *et al.*, 2011). Assuming that the variability
646 in the eCO₂ response of NPP during the first three years of the experiments was predominantly
647 influenced by meteorological conditions and not N availability (which is what most of the models
648 suggested), the weather-related standard error at Duke (1.3 %) is lower than the across ring
649 variations (3%), whereas it is higher at ORNL (2.9 % and 0.1%, respectively). These weather-
650 related variations add uncertainty to our estimates of the initial response of NPP to eCO₂, whereas
651 they appear small enough to allow to decipher the long-term trend, which we assessed as a 5 year
652 mean towards the end of the experiment. We cannot rule out, however, that extreme events such as
653 the ice storm at Duke in December 2002 (McCarthy *et al.*, 2007), have strongly altered the forest's
654 C-N dynamics and thereby obscured the expected trajectory of NPP enhancement. While the
655 models' meteorological forcing contained these extreme events, none of the models incorporated
656 the damage processes associated with for instance ice-break or wind damage.

657 A further complicating factor in the model-data analyses is that the magnitude of the N limitation of
658 the CO₂ response depends on various boundary conditions of the experiment, including the
659 magnitude of the CO₂-perturbation, and the pool of plant-available N at the beginning of the
660 experiment. The step-increase in CO₂ is much faster than projected future transient increases in
661 atmospheric CO₂. Thus, the experiment produces a suddenly increasing plant N demand (Luo &

662 Reynolds, 1999), which could (a) lead to an overestimate of the importance of nutrient constraints
663 and (b) trigger ecosystem processes that would not have occurred otherwise. The initial pool of
664 easily plant-accessible N, either in the form of mineral N or readily decomposable dead organic
665 material, is influenced by the land-use history of the plots. It is difficult to estimate from bulk soil
666 SOM measurements, as the net N mineralisation depends on the partitioning of SOM into pools
667 with different turnover times. In the absence of suitable initialisation data, most models generated
668 their initial condition based on site history, which caused uncertainty in the amount of net N
669 mineralisation and thus N availability for plants at the start of the experiment. Whether or not a
670 model simulates progressive N limitation, and at what time-scale, therefore depends not only on the
671 model structure, but also on the initialisation protocol. In particular, the ED2.1 model did not show
672 signs of N limitation, because it did not simulate N inputs or losses; so the prescribed initial SOM
673 pool provided ample inorganic N to support the growth of the trees throughout the simulation
674 period. To minimise the effect of initial conditions, the models were evaluated in terms of the
675 compatibility of their component processes with observations, rather than in terms of the average
676 modelled productivity and N uptake response to CO₂.

677

678 **5. Concluding remarks and recommendations for future experiments**

679 The two FACE experiments initially showed a similar productivity response to eCO₂, relative to a
680 comparable base-line, in terms of forest productivity and forest N-use as well as climate and
681 atmospheric N inputs. The long-term responses diverged strongly: the cumulated *NPP* response to
682 eCO₂ at the deciduous site was about half that of the evergreen site. The primary reason for this
683 difference was that altered soil organic matter dynamics increased plant N availability at Duke
684 forest at a rate that allowed the vegetation to maintain elevated levels of N uptake, whereas this did
685 not happen at a sufficient rate at ORNL FACE. Furthermore, a corollary of the different allocation
686 responses to eCO₂ was that almost the entire *NPP* enhancement remained in vegetation biomass in
687 Duke, whereas eCO₂ did not alter vegetation biomass at ORNL FACE.

688 Many models in the ensemble were capable of reproducing the observed initial increase of *NPP*
689 with eCO₂. However, in the majority of cases, this response resulted from compensating errors in
690 the underlying process responses, as the models did not correctly simulate the magnitude of the
691 observed initial increase in plant N uptake at both sites, and wrongly attributing a large share of the
692 increased *NPP* to enhanced nitrogen-use efficiency. This result cautions for a too simplistic model-
693 data comparison and underlines the necessity of the detailed process-level evaluation. Comparing
694 process responses of ecosystem models against the observations provided essential information on
695 model validity: we were able to identify component processes within particular models that were

696 operating well (qualitatively and quantitatively), even though the overall observed ecosystem eCO₂
697 response was not accurately reproduced.

698 Models with flexible stoichiometry and allocation patterns that respond to nitrogen stress captured
699 the qualitative responses observed at both sites. Ecosystem models with flexible tissue
700 stoichiometry predicted a larger CO₂-response of *NPP* response despite a lower than observed CO₂-
701 response of fN_{up} , and they generally overestimated the observed increase in vegetation C:N ratio.
702 Despite the conceptually increased accuracy of the results, this clearly shows that a more explicitly
703 process-based approach to modelling stoichiometric flexibility is to be important for capturing the
704 eCO₂ response at these sites.

705 Despite the diversity of the modelling approaches employed here, all 11 combinations of C-N cycle
706 processes include mechanisms consistent with the progressive nitrogen limitation hypothesis
707 (Comins & McMurtrie, 1993; Luo *et al.*, 2004), although the extent to which PNL was simulated
708 varied depending on the assumed tightness of the stoichiometric constraint and openness of the N
709 cycle. While this generally agrees with the observed trends at ORNL FACE, most models failed to
710 simulate the sustained *NPP* enhancement at the Duke FACE site, because the mechanisms to
711 increase N availability for plant growth included in these models are insufficient to explain the
712 observed increases. This tendency to underestimate the net transfer of N from soils to vegetation
713 under elevated CO₂ at Duke calls for a better representation of below-ground processes, in
714 particular root allocation and microbial responses to enhanced rhizodeposition.

715 Large uncertainty as to whether observed changes in aboveground N stocks are due to a
716 redistribution of N from soils or to newly acquired N stems from the low signal-to-noise ratio in soil
717 N inventories. Precise inventories well below the active rooting depth at the beginning of the
718 experiment (as it may increase as the experiment progresses) would help, as would additional
719 regular measurements of N balance components (N leaching and gaseous emission). Additional
720 experiments using open-top chambers may further help to reduce uncertainty with respect to the
721 below-ground mass balance and the net transfer of nutrients from soil to plants. Replicated factorial
722 manipulation of nutrient availability and atmospheric [CO₂] treatments could help to elucidate
723 process interactions regarding allocation and stoichiometric responses to altered C and N
724 availability. The strong increase in atmospheric CO₂ might have triggered processes that would not
725 have occurred, if CO₂ had increased at a more gradual pace. It would be of interest to investigate
726 nutrient responses in ecosystem-level experiments where CO₂ is elevated more gradually to the
727 maximum level, in instalments allowing the ecosystem to adjust at least partially to the new
728 conditions. To reduce the dependency of the experimental results on the initial state of the
729 ecosystem, it would also be desirable to conduct future elevated CO₂ experiments with replication

730 of different soil fertilities. This model comparison exercise has also underlined the increasingly
731 recognised need for data sets from large-scale experiments to be collated into a central, versioned
732 data repository that is readily accessible to modellers, if we are to fully capitalise on the potential
733 for such experiments to inform models.

734 The different responses of several key processes at the two experimental sites, which cannot be
735 explained by any of the models, imply that one should be sceptical of overarching statements
736 concerning the responses of ecosystems to increasing levels of atmospheric CO₂. There is currently
737 insufficient knowledge to fully constrain the eCO₂ response of global terrestrial ecosystem models,
738 despite the existing body of experimental evidence. Nevertheless, the ecosystem models were able
739 to capture important features of the experiments, lending some support to their projections (e.g.,
740 Thornton *et al.*, 2009; Zaehle *et al.*, 2010; Zhang *et al.*, 2011).

741

742 **Acknowledgements**

743 This study was conducted as a part of the ‘Benchmarking ecosystem response models with
744 experimental data from long-term CO₂ enrichment experiments’ Working Group supported by the
745 National Center for Ecological Analysis and Synthesis, a Center funded by NSF (Grant #EF-
746 0553768), the University of California, Santa Barbara and the State of California. The ORNL and
747 Duke FACE sites and additional synthesis activities were supported by the US Department of
748 Energy Office of Science, Biological and Environmental Research Program. In particular, Duke
749 FACE research was supported under grant number (FACE, DE-FG02-95ER62083). SZ was
750 supported by the FP7 people programme through grants’ no PERG02-GA-2007-224775 and
751 238366. MdK and BEM were supported by ARC Discovery Grant DP1094791, and TH by the
752 research funding programme “LOEWE-Landesoffensive zur Entwicklung wissenschaftlich-
753 ökonomischer Exzellenz” of Hesse's Ministry of Higher Education.

754

755 **References**

756 **Ainsworth EA, Long SP. 2005.** What have we learned from 15 years of free-air CO₂ enrichment
757 (FACE)? A meta-analytic review of the responses of photosynthesis, canopy properties and plant
758 production to rising CO₂. *New Phytologist* **165**: 351–372.

759 **Arora VK, Boer GJ, Freidlingstein P, Eby M, Jones CD, Christian JR, Bonan G, Bopp L,**
760 **Brovkin V, Cadule P, *et al.* 2013.** Carbon-concentration and carbon-climate feedbacks in CMIP5
761 Earth system models. *Journal of Climate* **26**: 5289–5314. doi: 10.1175-JCLI-D-12-00494.1.

- 762 **Arrhenius S. 1896.** On the influence of carbonic acid in the air upon the temperature of the ground.
763 *Philosophical Magazine and Journal of Science* **41**: 237–276.
- 764 **Bonan GB, Oleson KW, Fisher RA, Lasslop G, Reichstein M. 2012.** Reconciling leaf
765 physiological traits and canopy flux data: Use of the TRY and FLUXNET databases in the
766 Community Land Model version 4. *Journal of Geophysical Research* **117**: doi: 10.1029–
767 2011JG001913.
- 768 **Collatz GJ, Ball JT, Grivet C, Berry JA. 1991.** Physiological and environmental regulation of
769 stomatal conductance, photosynthesis and transpiration - a model that includes a laminar boundary
770 layer. *Agricultural and Forest Meteorology* **54**: 107–136.
- 771 **Comins H, McMurtrie RE. 1993.** Long-term biotic response of nutrient-limited forest ecosystems
772 to CO₂-enrichment: equilibrium behaviour of integrated plant-soil models. *Ecological Applications*
773 **3**: 666–681.
- 774 **Cramer W, Bondeau A, Woodward FI, Prentice IC, Betts RA, Brovkin V, Cox PM, Fisher V,
775 Foley JA, Friend AD, et al. 2001.** Global response of terrestrial ecosystem structure and function
776 to CO₂ and climate change: results from six dynamic global vegetation models. *Global Change*
777 *Biology* **7**: 357–373.
- 778 **Crous KY, Walters MB, Ellsworth DS. 2008.** Elevated CO₂ concentration affects leaf
779 photosynthesis–nitrogen relationships in *Pinus taeda* over nine years in FACE. *Tree Physiology* **28**:
780 607–614.
- 781 **De Kauwe M, Medlyn BE, Zaehle S, Walker AP, Dietze M, Thomas H, Jain AK, Luo Y,
782 Parton WJ, Prentice IC, et al. 2013.** Forest water use and water use efficiency at elevated CO₂: a
783 model-data intercomparison at two contrasting temperate forest FACE sites. *Global Change*
784 *Biology* **19**: 1759–1779.
- 785 **Drake JE, Darby BA, Giasson MA, Kramer MA, Phillips RP, Finzi AC. 2013.** Stoichiometry
786 constrains microbial response to root exudation- insights from a model and a field experiment in a
787 temperate forest. *Biogeosciences* **10**: 821–838.
- 788 **Drake JE, Gallet-Budynek A, Hofmockel KS, Bernhardt ES, Billings SA, Jackson RB,
789 Johnsen KS, Lichter J, McCarthy HR, McCormack ML, et al. 2011.** Increases in the flux of
790 carbon belowground stimulate nitrogen uptake and sustain the long-term enhancement of forest
791 productivity under elevated CO₂. *Ecology Letters* **14**: 349–357.

- 792 **Ellsworth DS, Thomas R, Crous KY, Palmroth S, Ward E, Maier C, DeLucia E, Oren R.**
793 **2011.** Elevated CO₂ affects photosynthetic responses in canopy pine and subcanopy deciduous trees
794 over 10 years: a synthesis from Duke FACE. *Global Change Biology* **18**: 223–242.
- 795 **Farquhar GD, Caemmerer SV, Berry JA. 1980.** A biochemical model of photosynthetic CO₂
796 assimilation in leaves of C₃ Species. *Planta* **149**: 78–90.
- 797 **Finzi AC, DeLucia E, Hamilton J, Schlesinger W, Richter D. 2002.** The nitrogen budget of a
798 pine forest under free air CO₂ enrichment. *Oecologia* **132**: 567–578.
- 799 **Finzi AC, Norby RJ, Calfapietra C, Gallet-Budynek A, Gielen B, Holmes WE, Hoosbeek MR,**
800 **Iversen CM, Jackson RB, Kubiske ME, et al. 2007.** Increases in nitrogen uptake rather than
801 nitrogen-use efficiency support higher rates of temperate forest productivity under elevated CO₂.
802 *Proceedings of the National Academy of Sciences* **104**: 14014–14019.
- 803 **Friend AD, Stevens AK, Knox RG, Cannell MGR. 1997.** A process-based, terrestrial biosphere
804 model of ecosystem dynamics (Hybrid v3.0). *Ecological Modelling* **95**: 249–287.
- 805 **Garten CT Jr, Iversen CM, Norby RJ. 2011.** Litterfall ¹⁵N abundance indicated declining soil
806 nitrogen availability in a free-air CO₂ enrichment experiment. *Ecology* **92**: 133–139.
- 807 **Harley PC, Loreto F, Marco GD, Sharkey TD. 1992.** Theoretical Considerations when
808 estimating the mesophyll conductance to CO₂ flux by analyses of the response of photosynthesis to
809 CO₂. *Plant Physiology* **98**: 1429–1436.
- 810 **Haxeltine A, Prentice IC. 1996.** A general model for the light-use efficiency of primary
811 production. *Functional Ecology* **10**: 551–561.
- 812 **Hickler Thomas, Smith B, Prentice IC, Mjofors K, Miller P, Arneth A, Sykes MT. 2008.** CO₂
813 fertilization in temperate FACE experiments not representative of boreal and tropical forests.
814 *Global Change Biology* **14**: 1531–1542.
- 815 **Hofmockel KS, Gallet-Budynek A, McCarthy HR, Currie WS, Jackson RB, Finzi AC. 2011.**
816 Sources of increased N uptake in forest trees growing under elevated CO₂: results of a large-scale
817 ¹⁵N study. *Global Change Biology* **17**: 3338–3350.
- 818 **Iversen CM. 2009.** Digging deeper: fine-root responses to rising atmospheric CO₂ concentration in
819 forested ecosystems. *New Phytologist* **186**: 346–357.

- 820 **Iversen CM, Hooker TD, Classen AT, Norby RJ. 2011.** Net mineralization of N at deeper soil
821 depths as a potential mechanism for sustained forest production under elevated [CO₂]. *Global*
822 *Change Biology* **17**: 1130–1139.
- 823 **Iversen CM, Keller JK, Garten CT Jr, Norby RJ. 2012.** Soil carbon and nitrogen cycling and
824 storage throughout the soil profile in a sweetgum plantation after 11 years of CO₂-enrichment.
825 *Global Change Biology* **18**: 1684–1697.
- 826 **Iversen CM, Ledford J, Norby RJ. 2008.** CO₂ enrichment increases carbon and nitrogen input
827 from fine roots in a deciduous forest. *New Phytologist* **179**: 837–847.
- 828 **Jastrow JD, Miller MR, Matamala R, Norby RJ, Boutton TW, Rice CW, Owensby CE. 2005.**
829 Elevated atmospheric carbon dioxide increases soil carbon. *Global Change Biology* **11**: 2057–2064.
- 830 **Johnson DW, Cheng W, Joslin JD, Norby RJ, Edwards NT, Todd DE. 2004.** Effects of elevated
831 CO₂ on nutrient cycling in a sweetgum plantation. *Biogeochemistry* **69**: 379–403.
- 832 **Kull O, Kruijt B. 1998.** Leaf photosynthetic light response: a mechanistic model for scaling
833 photosynthesis to leaves and canopies. *Functional Ecology* **12**: 767–777.
- 834 **Lasslop G, Reichstein M, Papale D, Richardson AD, Arneth A, Barr A, Stoy PC, Wohlfahrt**
835 **G. 2010.** Separation of net ecosystem exchange into assimilation and respiration using a light
836 response curve approach: critical issues and global evaluation. *Global Change Biology* **16**: 187–
837 208.
- 838 **Lichter J, Billings SA, Ziegler SE, Gaidh D, Ryals R, Finzi AC, Jackson RB, Stemmler EA,**
839 **Schlesinger WH. 2008.** Soil carbon sequestration in a pine forest after 9 years of atmospheric CO₂
840 enrichment. *Global Change Biology* **14**: 2910–2922.
- 841 **Liebig JV. 1843.** *Die Chemie in ihrer Anwendung auf Agricultur und Physiologie*. Braunschweig,
842 Deutschland: Verlag Vieweg.
- 843 **Luo Y, Reynolds JF. 1999.** Validity of extrapolating field CO₂ experiments to predict carbon
844 sequestration in natural ecosystems. *Ecology* **80**: 1568–1583.
- 845 **Luo Y, Su B, Currie WS, Dukes JS, Finzi AC, Hartwig U, Hungate BA, McMurtrie RE, Oren**
846 **R, Parton WJ, et al. 2004.** Progressive nitrogen limitation of ecosystem responses to rising
847 atmospheric carbon dioxide. *BioScience* **54**: 731–739.

- 848 **Maier CA, Palmroth S, Ward E. 2008.** Short-term effects of fertilization on photosynthesis and
849 leaf morphology of field-grown loblolly pine following long-term exposure to elevated CO₂
850 concentration. *Tree Physiology* **28**: 597–606.
- 851 **Maire V, Martre P, Kattge J, Gastal F, Esser G, Fontaine S, Soussana J-F. 2012.** The
852 coordination of leaf photosynthesis links C and N fluxes in C3 plant species. *PLoS ONE* **7**: e38345.
- 853 **McCarthy HR, Oren R, Finzi AC, Ellsworth DS, KIM H-S, Johnsen KH, Millar B. 2007.**
854 Temporal dynamics and spatial variability in the enhancement of canopy leaf area under elevated
855 atmospheric CO₂. *Global Change Biology* **13**: 2479–2497.
- 856 **McCarthy HR, Oren R, Johnsen KH, Gallet-Budynek A, Pritchard SG, Cook CW, LaDeau
857 SL, Jackson RB, Finzi AC. 2010.** Re-assessment of plant carbon dynamics at the Duke free-air
858 CO₂ enrichment site: interactions of atmospheric [CO₂] with nitrogen and water availability over
859 stand development. *New Phytologist* **185**: 514–528.
- 860 **McMurtrie RE, Dewar RC. 2013.** New insights into carbon allocation by trees from the
861 hypothesis that annual wood production is maximized. *New Phytologist* **199**: 981–990.
- 862 **McMurtrie RE, Norby RJ, Medlyn BE, Dewar RC, Pepper DA, Reich PB, Barton CVM.
863 2008.** Why is plant-growth response to elevated CO₂ amplified when water is limiting, but reduced
864 when nitrogen is limiting? A growth-optimisation hypothesis. *Functional Plant Biology* **35**: 521–
865 534.
- 866 **Medlyn BE. 1996a.** The optimal allocation of nitrogen within the C3 photosynthetic system at
867 elevated CO₂. *Australian Journal of Plant Physiology* **23**: 593–603.
- 868 **Medlyn BE. 1996b.** Interactive effects of atmospheric carbon dioxide and leaf nitrogen
869 concentration on canopy light use efficiency: a modeling analysis. *Tree Physiology* **16**: 201–209.
- 870 **Medvigy D, Wofsy SC, Munger JW, Hollinger DY, Moorcroft PR. 2009.** Mechanistic scaling of
871 ecosystem function and dynamics in space and time: Ecosystem Demography model version 2.
872 *Journal of Geophysical Research* **114**: G01002.
- 873 **Melillo JM, Butler S, Johnson J, Mohan J, Steudler P, Lux H, Burrows E, Bowles F, Smith R,
874 Scott L, et al. 2011.** Soil warming, carbon-nitrogen interactions, and forest carbon budgets.
875 *Proceedings of the National Academy of Sciences of the United States of America* **108**: 9508–9512.

- 876 **Norby R, Iversen CM. 2006.** Nitrogen uptake, distribution, turnover, and efficiency of use in a
877 CO₂ enriched sweetgum forest. *Ecology* **87**: 5–14.
- 878 **Norby RJ, DeLucia EH, Gielen B, Calfapietra C, Giardina CP, King JS, Ledford J,**
879 **McCarthy HR, Moore DJP, Ceulemans R, et al. 2005.** Forest response to elevated CO₂ is
880 conserved across a broad range of productivity. *Proceedings of the National Academy of Sciences of*
881 *the United States of America* **102**: 18052–18056.
- 882 **Norby RJ, Hanson PJ, O'Neill EG, Tschaplinski TJ, Hansen RA, Cheng W, Wullschleger SD,**
883 **Gunderson CA, Edwards NT, Johnson DW. 2002.** Net primary productivity of a CO₂-enriched
884 deciduous forest and the implications for carbon storage. *Ecological Applications* **12**: 1261–1266.
- 885 **Norby RJ, Todd DE, Fults J, Johnson DW. 2001.** Allometric determination of tree growth in a
886 CO₂-enriched sweetgum stand. *New Phytologist* **150**: 477–487.
- 887 **Norby RJ, Warren JM, Iversen CM, Medlyn BE, McMurtrie RE. 2010.** CO₂ enhancement of
888 forest productivity constrained by limited nitrogen availability. *Proceedings of the National*
889 *Academy of Sciences of the United States of America* **107**: 19368–19373.
- 890 **Oren R, Ellsworth DS, Johnsen KH, Phillips N, Ewers BE, Maier C, Schafer KVR, McCarthy**
891 **H, Hendrey G, McNulty SG, et al. 2001.** Soil fertility limits carbon sequestration by forest
892 ecosystems in a CO₂-enriched atmosphere. *Nature* **411**: 469–472.
- 893 **Palmroth S, Oren R, McCarthy HR, Johnsen KH, Finzi AC, Butnor JR, Ryan MG, Schlese U.**
894 **2006.** Aboveground sink strength in forests controls the allocation of carbon below ground and its
895 [CO₂] - induced enhancement. *Proceedings of the National Academy of Sciences* **103**: 19362–
896 19367.
- 897 **Parton WJ, Hanson PJ, Swanston C, Torn M, Trumbore SE, Riley W, Kelly R. 2010.** ForCent
898 model development and testing using the Enriched Background Isotope Study experiment. *Journal*
899 *of Geophysical Research* **115**: G04001.
- 900 **Piao SL, Sitch SA, Ciais P, Friedlingstein P, Peylin P, Wang X, Ahlström A, Anav A, Canadell**
901 **JG, Cong N, et al. 2013.** Evaluation of terrestrial carbon cycle models for their response to climate
902 variability and to CO₂ trends. *Global Change Biology* **19**: 2117–2132.
- 903 **Rastetter EB, Agren GI, Shaver GR. 1997.** Responses of N-limited ecosystems to increased CO₂:
904 A balanced-nutrition, coupled-element-cycles model. *Ecological Applications* **7**: 444–460.

- 905 **Rastetter EB, McKane RB, Shaver GR, Melillo JM. 1992.** Changes in C storage by terrestrial
906 ecosystems: How C-N interactions restrict responses to CO₂ and temperature. *Water, Air, and Soil*
907 *Pollution* **64**: 327–344.
- 908 **Sands PJ. 1995.** Modelling canopy production I. optimal distribution of photosynthetic resources.
909 *Australian Journal of Plant Physiology* **22**: 593–601.
- 910 **Sands PJ. 1996.** Modelling canopy production III. Canopy light-utilisation efficiency and its
911 sensitivity to physiological and environmental variables. *Australian Journal of Plant Physiology* **23**:
912 103–114.
- 913 **Sitch SA, Friedlingstein P, Gruber N, Jones S, Murray-Tortarolo G, Ahlström A, Doney SC,**
914 **Graven H, Heinze C, Huntingford C, et al. 2013.** Trends and drivers of regional sources and
915 sinks of carbon dioxide over the past two decades. **10**: 1–65.
- 916 **Sitch SA, Huntingford C, Gedney N, Levy PE, Lomas M, Piao SL, Betts R, Ciais P, Cox PM,**
917 **Friedlingstein P, et al. 2008.** Evaluation of the terrestrial carbon cycle, future plant geography and
918 climate-carbon cycle feedbacks using five Dynamic Global Vegetation Models (DGVMs). *Global*
919 *Change Biology* **14**: 2015–2039.
- 920 **Smith B, Prentice IC, Sykes MT. 2001.** Representation of vegetation dynamics in the modelling
921 of terrestrial ecosystems: comparing two contrasting approaches within European climate space.
922 *Global Ecology and Biogeography* **10**: 621–637.
- 923 **Smith B, Warlind D, Arneth A, Thomas H, Leadly P, Siltberg J, Zaehle S. 2013.** Implications
924 of incorporating N cycling and N limitations on primary production in an individual-based dynamic
925 vegetation model. *Biogeosciences Discussions* **10**: 18563–18611.
- 926 **Sokolov AP, Kicklighter DW, Melillo JM, Felzer BS, Schlosser CA, Cronin TW. 2008.**
927 Consequences of considering carbon-nitrogen interactions on the feedbacks between climate and
928 the terrestrial carbon cycle. *Journal of Climate* **21**: 3776–3796.
- 929 **Thornton PE, Zimmermann NE. 2007.** An improved canopy Integration scheme for a land
930 surface model with prognostic canopy structure. *Journal of Climate* **20**: 3902–3923.
- 931 **Thornton PE, Lamarque J-F, Rosenbloom NA, Mahowald NM. 2007.** Influence of carbon-
932 nitrogen cycle coupling on land model response to CO₂ fertilization and climate variability. *Global*
933 *Biogeochemical Cycles* **21**: GB4018.

- 934 **Thornton PE, S C Doney, K Lindsay, J K M, N Mahowald, J T Randerson, I Fung, J F**
935 **Lamarque, J J Feddema, Lee YH. 2009.** Carbon-nitrogen interactions regulate climate-carbon
936 cycle feedbacks: results from an atmosphere-ocean general circulation model. *Biogeosciences* **6**:
937 2099–2120.
- 938 **Vitousek PM, Howarth RW. 1991.** Nitrogen limitation on land and in the sea - how it can occur.
939 *Biogeochemistry* **13**: 87–115.
- 940 **Wang S, Grant RF, Verseghy DL, Black TA. 2001.** Modelling plant carbon and nitrogen
941 dynamics of a boreal aspen forest in CLASS — the Canadian Land Surface Scheme. *Ecological*
942 *Modelling* **142**: 135–154.
- 943 **Wang Y-P, Kowalczyk E, Leuning R, Abramowitz G, Raupach MR, Pak B, van Gorsel E,**
944 **Luhar A. 2011.** Diagnosing errors in a land surface model (CABLE) in the time and frequency
945 domains. *Journal of Geophysical Research* **116**: G01034.
- 946 **Wang YP, Law RM, Pak B. 2010.** A global model of carbon, nitrogen and phosphorus cycles for
947 the terrestrial biosphere. *Biogeosciences* **7**: 2261–2282.
- 948 **Warren JM, Pötzelsberger E, Wullschleger SD, Thornton PE, Hasenauer H, Norby RJ. 2011.**
949 Ecohydrologic impact of reduced stomatal conductance in forests exposed to elevated CO₂.
950 *Ecohydrology* **4**: 196–210.
- 951 **Weng E, Luo Y. 2008.** Soil hydrological properties regulate grassland ecosystem responses to
952 multifactor global change: A modeling analysis. *Journal of Geophysical Research* **113**: G03003.
- 953 **Woodward FI, Smith TM, Emanuel WR. 1995.** A global land primary productivity and
954 phytogeography model. *Global Biogeochemical Cycles* **9**: 471–490.
- 955 **Xu C, Fisher R, Wullschleger SD, Wilson CJ, Cai M, McDowell NG. 2012.** Toward a
956 mechanistic modeling of nitrogen limitation on vegetation dynamics. *PLoS ONE* **7**: e37914.
- 957 **Yang X, Wittig V, Jain AK, Post W. 2009.** The integration of nitrogen cycle dynamics into the
958 Integrated Science Assessment Model (ISAM) for the study of terrestrial ecosystem responses to
959 global change. *Global Biogeochemical Cycles* **23**: GB4029 doi:10.1029–2009GB003474.
- 960 **Zaehle S, Dalmonech D. 2011.** Carbon–nitrogen interactions on land at global scales: current
961 understanding in modelling climate biosphere feedbacks. *Current Opinion in Environmental*
962 *Sustainability* **3**: 311–320.

963 **Zaehle S, Friend AD. 2010.** Carbon and nitrogen cycle dynamics in the O-CN land surface model:
964 1. Model description, site-scale evaluation, and sensitivity to parameter estimates. *Global*
965 *Biogeochemical Cycles* **24**: GB 1005.

966 **Zaehle S, Ciais P, Friend AD, Prieur V. 2011.** Carbon benefits of anthropogenic reactive nitrogen
967 offset by nitrous oxide emissions. *Nature Geoscience* **4**: 1–5.

968 **Zaehle S, Friedlingstein P, Friend AD. 2010.** Terrestrial nitrogen feedbacks may accelerate future
969 climate change. *Geophysical Research Letters* **37**: L01401.

970 **Zhang Q, Wang YP, Pitman AJ, Dai YJ. 2011.** Limitations of nitrogen and phosphorous on the
971 terrestrial carbon uptake in the 20th century. *Geophysical Research Letters* **38**: GL049244.

972

973 **Figure captions**

974 **Figure 1:** Conceptual diagram of the major nitrogen and carbon flows and stores in a terrestrial
 975 ecosystem. Blue arrows denote C fluxes and red arrows N fluxes between major plant
 976 compartments (green) and soil pools (black). Numbers 1-5 mark important carbon-nitrogen cycle
 977 linkages as described in Section 2.2: **1:** N-based GPP (GPP_N): the return of C assimilates per
 978 unit canopy N (eqn. 1); **2:** whole-plant nutrient use efficiency (NUE): the total amount of foliar,
 979 root, and woody production per unit of N taken up by plants. This process depends on the
 980 allocation of growth between different plant compartments (e.g. leaves, fine roots and wood) and
 981 the C:N stoichiometry of each compartment (eqn. 2); **3:** Plant N uptake (fN_{up}): the capacity of the
 982 plants to take up N from the soil (eqn. 4a). The plant-available soil N is determined by two
 983 factors: **4:** net N mineralisation (fN_{min}): the amount of N liberated from organic material through
 984 decomposition, which varies with microbial activity and litter quality (eqn. 4c); and **5:** the net
 985 ecosystem nitrogen exchange (NNE), based on N inputs from biological N fixation (fN_{fix}) and
 986 atmospheric deposition (fN_{dep}) and N losses from the ecosystem due to leaching to groundwater
 987 (fN_{leach}) and gaseous emission (fN_{gas}) (eqn. 4b). As an emergent property, the net amount of C
 988 that can be stored in an ecosystem following an increase in CO_2 depends on the eCO_2 effect on
 989 the ecosystem's N balance and the whole-ecosystem stoichiometry, which in turn depends on the
 990 change of the C:N stoichiometry of vegetation and soil, as well as partitioning of N between
 991 vegetation and soil (Rastetter *et al.*, 1992).

992 **Figure 2:** Ambient Net Primary Production (NPP ; a,b) and its response to elevated CO_2 (c,d) at the
 993 Duke (a,c) and ORNL (b,d) FACE experiments. The observations are across-plot averages, and
 994 the error bars denote ± 1 standard error.

995 **Figure 3:** Ambient plant N uptake (fN_{up} ; a,b) and its response to elevated CO_2 (c,d) at the Duke
 996 (a,c) and ORNL (b,d) FACE experiments. The observations are across-plot averages, and the
 997 error bars denote ± 1 standard error.

998 **Figure 4:** Ambient whole-plant nitrogen-use efficiency (NUE ; a,b) and its response to elevated CO_2
 999 (c,d) at the Duke (a,c) and ORNL (b,d) FACE experiments. The observations are across-plot
 1000 averages, and the error bars denote ± 1 standard error.

1001 **Figure 5:** First year response of net primary production (NPP) to elevated CO_2 (a,b) and the change
 1002 between the first year and the final five years of the experiment (c,d) at the Duke and ORNL
 1003 FACE sites, respectively, as well as the response of plant N uptake (fN_{up}) and whole-plant N-use
 1004 efficiency (NUE). The grey boxes denote the mean observed eCO_2 response ± 1 standard error.

1005 **Figure 6:** First year response of N-based NPP (NPP_N) to elevated CO_2 (a,b) and the change
 1006 between the first year and the final five years of the experiment (c,d) at the Duke FACE and
 1007 ORNL FACE sites, respectively, as well as the response of plant C-use efficiency (CUE), N-
 1008 based GPP (GPP_N) and canopy N, expressed as total canopy N (N_{can}) and foliar N concentration
 1009 (n_{can}). The grey boxes denote the mean observed eCO_2 response ± 1 standard error, where
 1010 observations corresponding to model output are available.

1011 **Figure 7:** Change in N-use efficiency of biomass production (NUE) at Duke (a) and ORNL (b)
 1012 FACE sites, integrated over the entire length of the experiment (1997-2005 and 1998-2008 for
 1013 Duke and ORNL FACE, respectively). ΔNUE_{alloc} denotes the change in NUE attributed to
 1014 changes allocation to leaves, fine roots, and wood, whereas, ΔNUE_{stoch} denotes the change in
 1015 NUE due to altered tissue C:N. The error bars denote ± 1 standard error.

1016 **Figure 8:** Cumulative plant N uptake due to eCO_2 over the length of the experiment, and its
 1017 attribution to different mechanisms according to eqn. 4 and 5 at the Duke (a) and ORNL (b)
 1018 FACE sites. Positive values indicate an increase in plant N uptake, negative a decline. (c-e)
 1019 Exemplary time courses of the net N balance for Duke forest, as predicted by CABLE (c), CLM4
 1020 (d), and O-CN (e). ΔfN_{up} : plant nitrogen uptake, $\Delta \tau_{N_{som}}$: change in net N mineralisation due to a
 1021 change in the soil organic N turnover time relative to the soil organic C turnover time; ΔN_{SOM} :
 1022 change in net N mineralisation due to a change in the organic N pool; ΔNNE change in the
 1023 ecosystem N balance (sum of N increases from biological N fixation and atmospheric N
 1024 deposition and N losses to leaching and gaseous emissions); ΔN_{inorg} : changes in the inorganic N
 1025 pool. The error bars on observations denote ± 1 standard error.

1026 **Figure 9:** Total change in ecosystem C due to eCO_2 at the Duke (a) and ORNL (b) FACE sites
 1027 resulting from changes in the total organic ecosystem N store (ΔN_{org}), vegetation and soil C:Ns
 1028 ($\Delta C:N_{veg}$ and $\Delta C:N_{soil}$), as well as changes in the fractionation of total ecosystem N between
 1029 vegetation and soil, measured as the fraction of total ecosystem N in vegetation ($f_{veg} = N_{veg}/N_{org}$).
 1030 The error bars denote ± 1 standard error.

1031 **Figure S1:** Cumulative effect of eCO_2 on C and N storage in the Duke and ORNL FACE sites.

1032

1033

1034

1035

1036

1037 **Appendix**

1038 **Table A1:** Overview of the models used and the representation of key processes in the carbon-
1039 nitrogen cycle.

1040 Footnote of Table A1: AET: actual evapotranspiration; C: Carbon; GPP: Gross Primary Production;

1041 N: Nitrogen; NPP: Net Primary Production; P: Phosphorous; R_a : Autotrophic Respiration; T:

1042 Temperature; $f(x)$: is a function of x . ¹: see (M.G. De Kauwe *et al.*, unpublished.) for details.

1043

Table A1: Overview of the models used and the representation of key processes in the carbon-nitrogen cycle.

| | | CABLE | CLM4 | DAYCENT | EALCO |
|---------------------|--|--|---|---|--|
| Key reference | | Wang <i>et al.</i> (2010, 2011) | Thornton & Zimmermann (2007); Thornton <i>et al.</i> (2007) | Parton <i>et al.</i> (2010) | Wang <i>et al.</i> (2001) |
| Time-step | | 30-min | 30-min | 1-day | 30-min |
| Plant C acquisition | Assimilation (GPP) | Farquhar <i>et al.</i> (1980) | Collatz <i>et al.</i> (1991) | 2 x NPP_{act} | Farquhar <i>et al.</i> (1980) |
| | N dependency of gross photosynthesis | $f(\text{leaf } N)$ | NPP_{act}/NPP_{pot} | None | $f(\text{leaf } N)$ |
| | Autotrophic respiration | $f(\text{tissue } N, T) + f(\text{growth rate})$ | $f(\text{tissue } C, T) + f(\text{growth rate})$ | 0.5 x GPP | $f(\text{tissue } C, T) + f(\text{growth rate})$ |
| | N dependency of whole-plant growth (if not $GPP - R_a$) | None | Potential growth (NPP_{pot}) limited by stoichiometric N requirement for new tissue growth | Potential growth ($f(\text{PAR}, T, \text{moisture}, \text{CO}_2)$) limited by stoichiometric N requirement for new tissue growth | None |
| Plant N acquisition | Nitrogen fixation | Prescribed based on Wang & Houlton (2009) | $f(NPP)$ | Plant associated N fixation: $f(N:P, \text{plant } N \text{ demand})$; soil N fixation: $f(AET)$ | None |
| | Nitrogen uptake | $f(\text{plant } N \text{ demand}, \text{soil } N \text{ availability})$ | $f(\text{relative strength of plant and microbial } N \text{ demand}, \text{inorganic } N \text{ pool size})$ | $f(\text{root biomass}, \text{plant demand}, \text{soil } N \text{ availability})$ | Competition of soil mineral N between plant and microbial |
| Plant growth | Allocation principle ¹ | Fixed allocation fractions, which vary according to phenological state | Fixed allocation fractions, derived from observations at the sites. | Hierarchical allocation factors, in which fine roots have priority over leaves and over wood, with prescribed maximum pool sizes | Fixed allocation fractions, which vary according to phenological state |
| | Maximum leaf area ¹ | Prescribed (LAI = 8; excess C is allocated to wood & roots) | Predicted | Predicted | Prescribed from observations at the site |
| | N effect on allocation ¹ | None | None | Nitrogen stress increases root allocation | None |
| | Plant tissue C:N stoichiometry | Flexible within 10% of the prescribed mean C:N | Fixed | Flexible within prescribed bounds | Flexible within prescribed bounds |

| | | CABLE | CLM4 | DAYCENT | EALCO |
|--------------------|---|---|---|---|--|
| Plant N turnover | N effect on turnover/mortality | None | Indirect via changes in NPP | Leaf turnover increases linearly with leaf N concentration | None |
| | N retention on leaf & root shedding | 50% of leaf N, 10% of root N | Litter has a fixed C:N (PFT specific) | 50% of leaf N | Retaining ratio depends on current tissue C:N ratio |
| Soil N turnover | SOM decay (other than dependent on soil T and moisture) | 3 litter pools (metabolic, structural, coarse woody debris), 3 SOM pools with different turnover times, 1 st order decay | 3 litter pools, 4 SOM pools, all with different turnover times, 1 st order decay | 3 litter pools (above and below ground combined), 4 SOM pools, all with different turnover times, 1 st order decay | 3 litter pools; 4 SOM pools with different turnover rates, 1 st order decay |
| | N effect on decomposition | Lignin:N ratio affects microbial efficiency and decomposition rate. Available soil mineral N constrains immobilization | Litter decomposition constrained by available soil N | Lignin:N ratio affects microbial efficiency and decomposition rate. Available soil mineral N constrains immobilization | Litter decomposition constrained by available soil N |
| | Soil C:N stoichiometry | Fixed for each pool | Fixed for each pool | f(mineral N concentration, within bounds) | f(mineral N concentration, within bounds) |
| Ecosystem N losses | N leaching | Proportional to mineral N pool | f(soil water N concentration, drainage) | DON + N leaching = f(precipitation, NO ₃ pool size) | f(mineral N concentration, drainage and surface runoff) |
| | N volatilisation | Proportional to net N mineralisation rate | Proportional to gross N mineralisation + 10% of mineral N remaining in the soil | NO _x , N ₂ O, N ₂ fluxes, as a function of soil N pool size, temperature, water | None |

Table A1: Overview of the models used and the representation of key processes in the carbon-nitrogen cycle

| | | ED2.1 | GDAY | ISAM | LPJ-GUESS |
|---------------------|---|---|---|--|--|
| Key reference | | Medvigy <i>et al.</i> (2009) | Comins & McMurtrie (1993) | Yang <i>et al.</i> (2009) | Smith <i>et al.</i> (2001; 2013) |
| Time-step | | 15-min | 1-day | 30-min | 1-day |
| Plant C acquisition | Assimilation | Farquhar <i>et al.</i> (1980) | Sands <i>et al.</i> (1995, 1996) | Farquhar <i>et al.</i> (1980) | Collatz <i>et al.</i> (1991) Haxeltine & Prentice (1996) |
| | N dependency of gross photosynthesis | None | $f(\text{leaf N})$ | Stoichiometric downregulation of v_{cmax} | $f(\text{leaf N})$ |
| | Autotrophic respiration | $f(\text{tissue C, T}) + f(\text{GPP})$ | 0.5 x GPP | $f(\text{tissue N, T})$ | $f(\text{tissue N, T}) + f(\text{GPP})$ |
| | N dependency of whole-plant growth (if not $\text{GPP} - R_a$) | Potential growth limited by stoichiometric N requirement for new tissue growth | None | None | None |
| Plant N acquisition | Nitrogen fixation | None | Prescribed | Predicted | Prescribed |
| | Nitrogen uptake | $f(\text{root biomass, plant N demand, soil N availability})$ | Fixed proportion of the inorganic N pool size | Michaelis-Menten Kinetics, increases with increased plant N demand | $f(\text{plant N demand, soil T})$ |
| Plant growth | Allocation principle ¹ | Functional relationships amongst leaf and sapwood (pipe-model), and sapwood and fine root biomass | Fixed allocation fractions, derived from observations at the sites. | Dynamic allocation fractions, based on light, water and phenology | Functional relationships amongst leaf and sapwood (pipe-model), and leaf and fine root biomass |
| | Maximum leaf area ¹ | Predicted | Predicted | Predicted | Predicted |
| | N effect on allocation ¹ | Nitrogen stress decreases leaf:root ratio | None | None | Nitrogen stress decreases leaf:root ratio |
| | Plant C:N stoichiometry | Fixed | Flexible | Flexible within prescribed bounds | Flexible within prescribed bounds |

| | | ED2.1 | GDAY | ISAM | LPJ-GUESS |
|--------------------|---|---|--|--|---|
| Plant N turnover | N effect on turnover/mortality | Indirect via changes in NPP | None | Indirect via changes in NPP | Indirect via changes in NPP |
| | N retention on leaf & root shedding | 50 % of N is retained with leaf fall, but 0% with root turnover. | 50 % of N is retained with leaf fall, but 0% with root turnover. | Biome dependent | 50% of N is retained |
| Soil N turnover | SOM decay (other than dependent on soil T and moisture) | three SOM pools with varying turnover rates. | 4 litter pools (above/below metabolic and structural litter) and three SOM pools with varying turnover rates. | 4 litter/SOM above ground pools, 4 litter/SOM below ground pools and one inert organic matter pool with different turnover rates | 5 litter pools (above/below metabolic and structural litter, plus an above CWD litter pool) and 5 SOM pools with varying turnover rates |
| | N effect on decomposition | litter decomposition constrained by available soil N | Lignin:N ratio affects microbial efficiency and decomposition rate. Available soil mineral N constrains immobilization | litter decomposition constrained by available soil N | litter decomposition constrained by available soil N |
| | Soil C:N stoichiometry | Fast pool: function of mineral N. Slow and Structural pool: Fixed C:N | f(mineral N concentration, within bounds) | Fixed | f(mineral N concentration, within bounds) |
| Ecosystem N losses | N leaching | None | Fixed proportion of the inorganic N pool size. | f(N pools size, drainage) | f(mineral N concentration, drainage) |
| | N volatilisation | None | None | NH ₃ volatilisation and denitrification losses | None |

Table A1: Overview of the models used and the representation of key processes in the carbon-nitrogen cycle

| | | OCN | SDGVM | TECO |
|---------------------|---|--|---|--|
| | Key reference | Zaehle & Friend (2010) | Woodward <i>et al.</i> (1995) | Weng & Luo (2008) updated |
| Times-step | | 30-min | 1-day | 30-min |
| Plant C acquisition | Assimilation | Farquhar <i>et al.</i> (1980) Kull & Kruijt (1998) | Farquhar <i>et al.</i> (1980) Harley <i>et al.</i> (1992) | Farquhar <i>et al.</i> (1980) |
| | N dependency of gross photosynthesis | $f(\text{leaf N})$ | $f(\text{leaf N})$ | $f(\text{leaf N})$ |
| | Autotrophic respiration | $f(\text{tissue N}) + f(\text{growth rate}) + \text{excess respiration if labile C exceeds storage capacity, in the limits of the labile C pool size}$ | $f(\text{tissue N, T})$ | $f(\text{leaf area, root and sapwood C})$ |
| | N dependency of whole-plant growth (if not $\text{GPP} - R_a$) | $f(\text{labile C pool size, stoichiometric N requirement for new tissue growth})$ | None | Surplus C under N stress is allocated to woody biomass. |
| Plant N acquisition | Nitrogen fixation | Prescribed | None | Prescribed |
| | Nitrogen uptake | Michaelis-Menten Kinetics, proportional to root biomass, increases with increased plant N demand | $f(\text{soil organic C and N})$ | $f(\text{root C, plant N demand})$ |
| Plant growth | Allocation principle ¹ | Functional relationships amongst leaf and sapwood (pipe-model), and leaf and fine root biomass | leaf allocation determined as C balance of lowest LAI layer of the previous year. Root & wood allocation fixed fraction if $\text{GPP} > 0$ | Resource limitations approach, prioritising leaf over root and wood allocation |
| | Maximum leaf area ¹ | Predicted | Predicted | Prescribed per plant functional type |
| | N effect on allocation ¹ | Increased plant N demand increases root:leaf ratio | None | N limitation increases allocation to woody biomass |
| | Plant C:N stoichiometry | Flexible within prescribed bounds | Foliar N is prescribed from observations | Flexible within prescribed narrow bounds |

| | | OCN | SDGVM | TECO |
|--------------------|---|--|---|---|
| Plant N turnover | N effect on turnover/mortality | Indirect via changes in NPP | None | None |
| | N retention on leaf & root shedding | 50% of N is retained | None | 50% of N is retained |
| Soil N turnover | SOM decay (other than dependent on soil T and moisture) | 3 litter pools; 4 SOM pools with different turnover times, 1 st order decay | 4 litter pools, 4 SOM pools, with different turnover times, 1 st order decay | 5 SOM pools (metabolic litter, structural litter, fast SOM, slow SOM, and passive SOM) with different turnover rates, 1 st order decay |
| | N effect on decomposition | Lignin:N ratio affects microbial efficiency and decomposition rate. Available soil mineral N constrains immobilization | n.a. | |
| | Soil C:N stoichiometry | f(mineral N concentration, within bounds) | Fixed | Flexible soil C:N ratios |
| Ecosystem N losses | N leaching | f(mineral N concentration, drainage) | None | f(mineralized N, runoff) |
| | N volatilisation | f(mineral N concentration, soil T, moisture and respiration) | None | Fixed proportion of mineral N, regulated by soil T |

Table A2: List of variable names used, as well as their description and unit. Tissue types considered are foliage (*f*), fine roots (*r*) and woody (*w*) biomass. C: Carbon; N: Nitrogen; DW: dry weight

| Variable | Description | Unit |
|--------------|---|---|
| a_i | fractional allocation to tissue type <i>i</i> | -- |
| B_i | Biomass of tissue type <i>i</i> | g DW m ⁻² |
| C_{org} | Ecosystem organic carbon | g C m ⁻² |
| C_{SOM} | Soil organic matter carbon (including the litter layer) | g C m ⁻² |
| C_{veg} | Vegetation carbon | g C m ⁻² |
| CUE | Carbon-use efficiency (NPP/GPP) | -- (g C yr ⁻¹ g ⁻¹ C yr) |
| GPP | Area-based gross primary production | g C m ⁻² yr ⁻¹ |
| GPP_N | N-based gross primary production | g C g ⁻¹ N _{can} yr ⁻¹ |
| fN_{dep} | Atmospheric nitrogen deposition | g N m ⁻² yr ⁻¹ |
| fN_{fix} | Biological nitrogen fixation | g N m ⁻² yr ⁻¹ |
| fN_{gas} | Ecosystem loss of nitrogen through gaseous emission | g N m ⁻² yr ⁻¹ |
| fN_{leach} | Ecosystem loss of nitrogen through leaching | g N m ⁻² yr ⁻¹ |
| fN_{min} | Net nitrogen mineralisation | g N m ⁻² yr ⁻¹ |
| fN_{up} | Plant nitrogen uptake | g N m ⁻² yr ⁻¹ |
| f_{trans} | Fraction of tissue N translocated before abscission | -- |
| f_{veg} | Fraction of organic ecosystem nitrogen in vegetation | -- |
| n_i | Nitrogen concentration of tissue type <i>i</i> | g N g ⁻¹ DW |
| N_{can} | Canopy nitrogen | g N m ⁻² |
| N_{org} | Ecosystem organic nitrogen | g N m ⁻² |
| N_{inorg} | Inorganic nitrogen in the ecosystem | g N m ⁻² |
| N_{SOM} | Soil organic matter nitrogen (including the litter layer) | g N m ⁻² |
| N_{veg} | Vegetation nitrogen | g N m ⁻² |
| NNE | Net ecosystem nitrogen exchange | g N m ⁻² yr ⁻¹ |
| NPP | Area-based Net primary production | g C m ⁻² yr ⁻¹ |
| NPP_N | N-based net primary production | g C g ⁻¹ N _{can} yr ⁻¹ |

| | | |
|------------------|--|--|
| NUE | Nitrogen-use efficiency (NPP/fN_{up}) | $\text{g C yr}^{-1} \text{ g}^{-1} \text{ N yr}$ |
| R_a | Autotrophic respiration | $\text{g C m}^{-2} \text{ yr}^{-1}$ |
| $\tau_{N_{veg}}$ | turnover time of nitrogen in vegetation | yr^{-1} |
| $\tau_{N_{SOM}}$ | turnover time of nitrogen in soil organic matter (including the litter layer) | yr^{-1} |

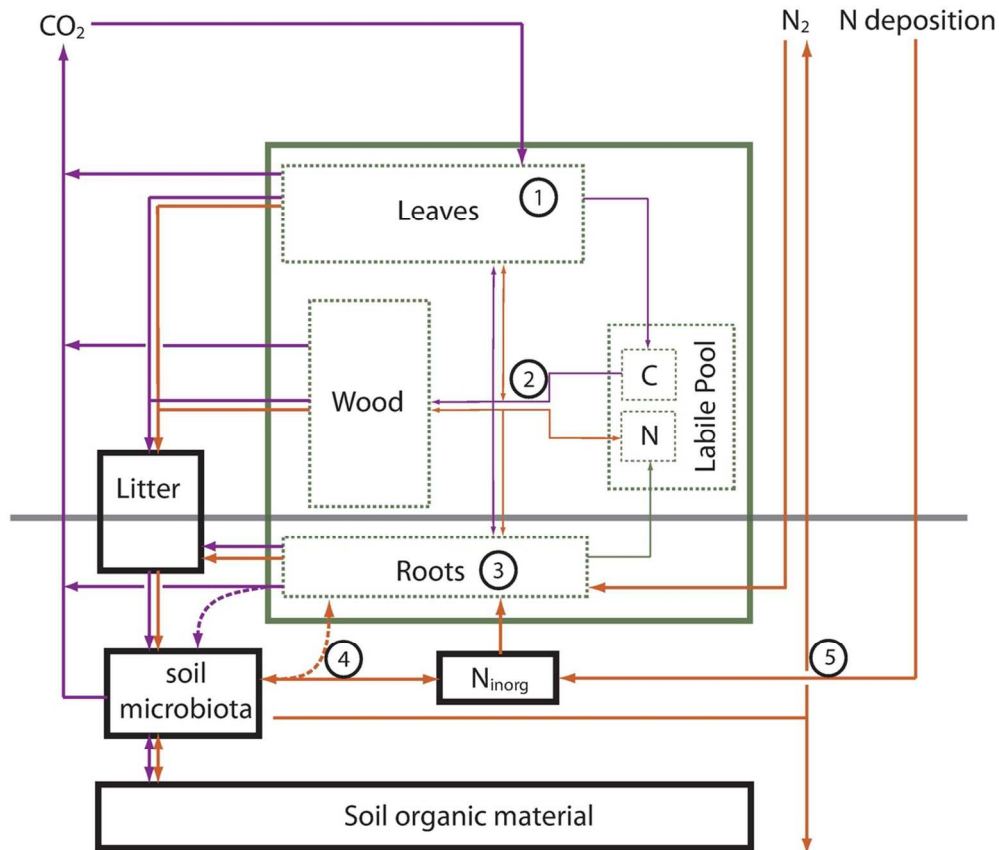


Figure 1: Conceptual diagram of the major nitrogen and carbon flows and stores in a terrestrial ecosystem. Blue arrows denote C fluxes and red arrows N fluxes between major plant compartments (green) and soil pools (black). Numbers 1-5 mark important carbon-nitrogen cycle linkages as described in Section 2.2: 1: N-based GPP (GPPN): the return of C assimilates per unit canopy N (eqn. 1); 2: whole-plant nutrient use efficiency (NUE): the total amount of foliar, root, and woody production per unit of N taken up by plants. This process depends on the allocation of growth between different plant compartments (e.g. leaves, fine roots and wood) and the C:N stoichiometry of each compartment (eqn. 2); 3: Plant N uptake (fN_{up}): the capacity of the plants to take up N from the soil (eqn. 4a). The plant-available soil N is determined by two factors: 4: net N mineralisation (fN_{min}): the amount of N liberated from organic material through decomposition, which varies with microbial activity and litter quality (eqn. 4c); and 5: the net ecosystem nitrogen exchange (NNE), based on N inputs from biological N fixation (fN_{fix}) and atmospheric deposition (fN_{dep}) and N losses from the ecosystem due to leaching to groundwater (fN_{leach}) and gaseous emission (fN_{gas}) (eqn. 4b). As an emergent property, the net amount of C that can be stored in an ecosystem following an increase in CO_2 depends on the eCO_2 effect on the ecosystem's N balance and the whole-ecosystem stoichiometry, which in turn depends on the change of the C:N stoichiometry of vegetation and soil, as well as partitioning of N between vegetation and soil (Rastetter et al., 1992).

102x86mm (300 x 300 DPI)

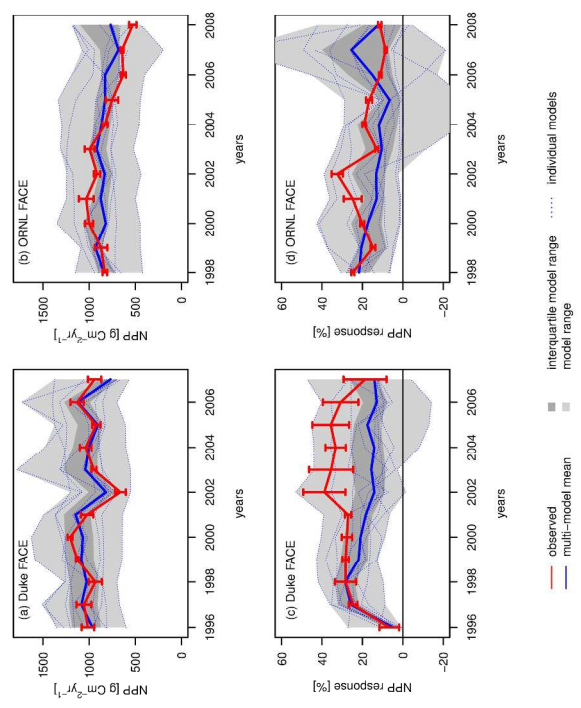


Figure 2: Ambient Net Primary Production (NPP; a,b) and its response to elevated CO₂ (c,d) at the Duke (a,c) and ORNL (b,d) FACE experiments. The observations are across-plot averages, and the error bars denote ± 1 standard error.
279x361mm (300 x 300 DPI)

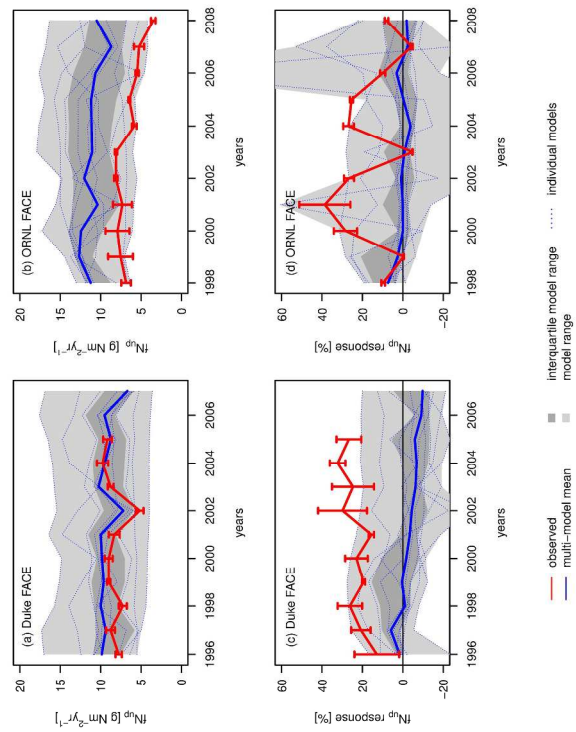


Figure 3: Ambient plant N uptake (fNup; a,b) and its response to elevated CO₂ (c,d) at the Duke (a,c) and ORNL (b,d) FACE experiments. The observations are across-plot averages, and the error bars denote ± 1 standard error.
279x361mm (300 x 300 DPI)

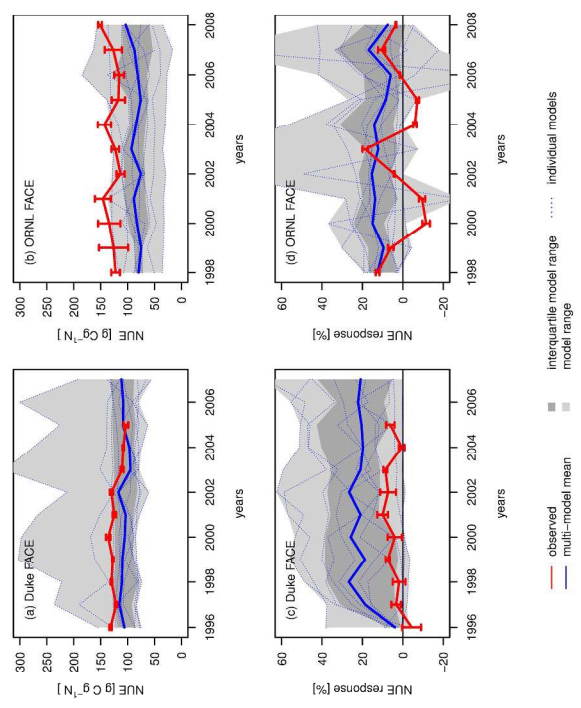


Figure 4: Ambient whole-plant nitrogen-use efficiency (NUE; a,b) and its response to elevated CO_2 (c,d) at the Duke (a,c) and ORNL (b,d) FACE experiments. The observations are across-plot averages, and the error bars denote ± 1 standard error.
279x361mm (300 x 300 DPI)

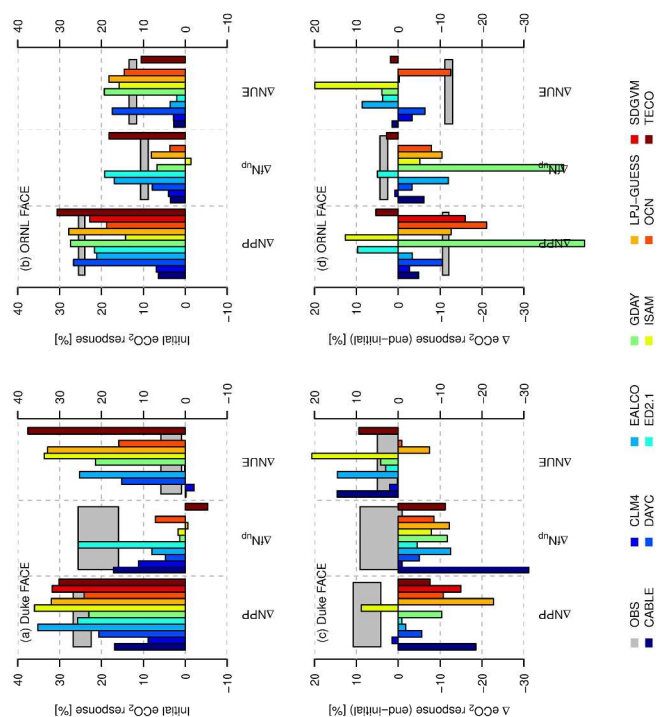


Figure 5: First year response of net primary production (NPP) to elevated CO₂ (a,b) and the change between the first year and the final five years of the experiment (c,d) at the Duke and ORNL FACE sites, respectively, as well as the response of plant N uptake (fNup) and whole-plant N-use efficiency (NUE). The grey boxes denote the mean observed eCO₂ response ± 1 standard error.

279x361mm (300 x 300 DPI)

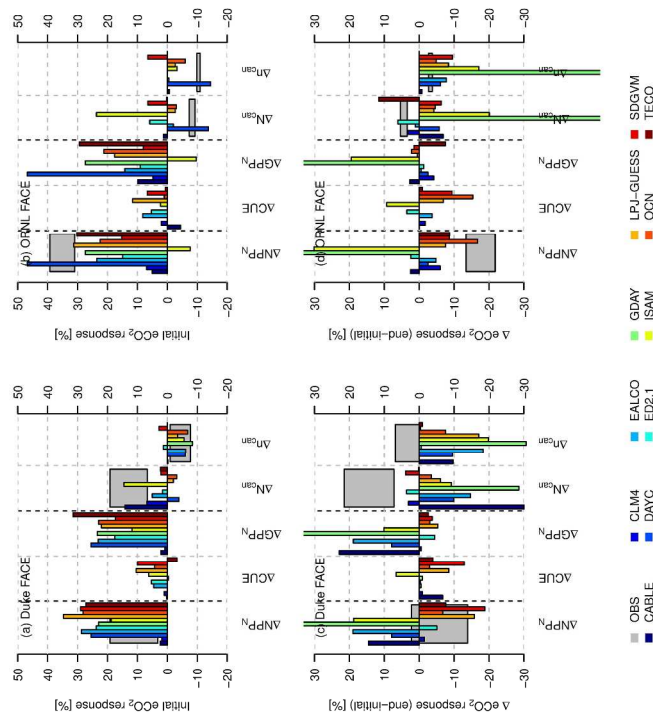


Figure 6: First year response of N-based NPP (NPPN) to elevated CO₂ (a,b) and the change between the first year and the final five years of the experiment (c,d) at the Duke FACE and ORNL FACE sites, respectively, as well as the response of plant C-use efficiency (CUE), N-based GPP (GPPN) and canopy N, expressed as total canopy N (N_{can}) and foliar N concentration (n_{can}). The grey boxes denote the mean observed eCO₂ response ± 1 standard error, where observations corresponding to model output are available.
279x361mm (300 x 300 DPI)

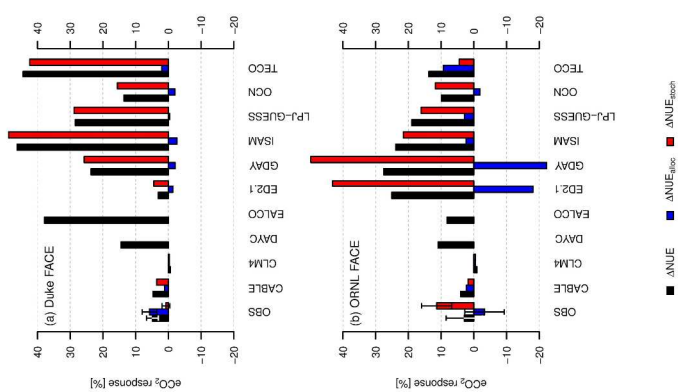


Figure 7: Change in N-use efficiency of biomass production (NUE) at Duke (a) and ORNL (b) FACE sites, integrated over the entire length of the experiment (1997-2005 and 1998-2008 for Duke and ORNL FACE, respectively). $\Delta\text{NUE}_{\text{alloc}}$ denotes the change in NUE attributed to changes allocation to leaves, fine roots, and wood, whereas, $\Delta\text{NUE}_{\text{stoch}}$ denotes the change in NUE due to altered tissue C:N. The error bars denote ± 1 standard error.

279x361mm (300 x 300 DPI)

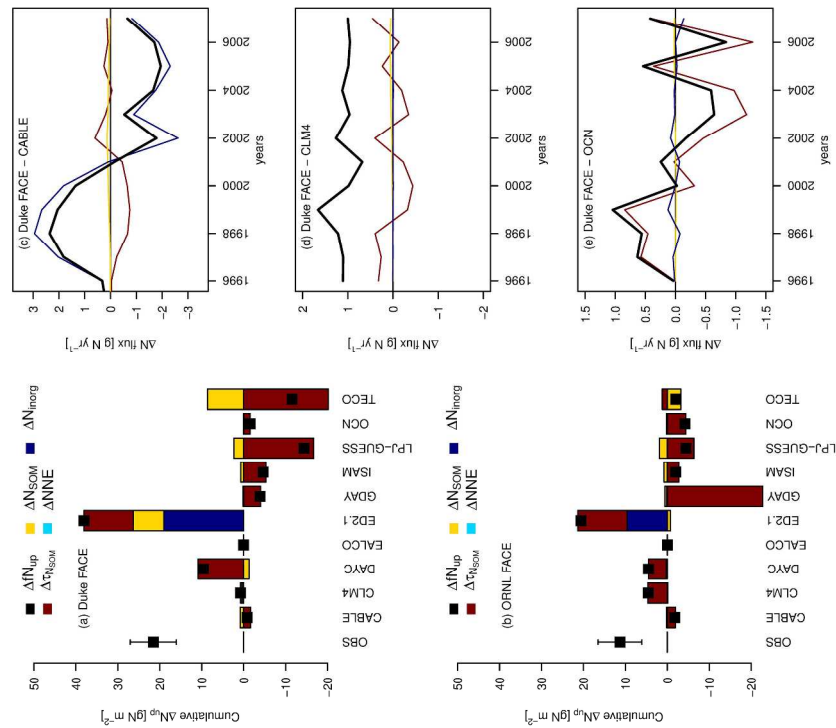


Figure 8: Cumulative plant N uptake due to eCO₂ over the length of the experiment, and its attribution to different mechanisms according to eqn. 4 and 5 at the Duke (a) and ORNL (b) FACE sites. Positive values indicate an increase in plant N uptake, negative a decline. (c-e) Exemplary time courses of the net N balance for Duke forest, as predicted by CABLE (c), CLM4 (d), and O-CN (e). ΔfN_{up} : plant nitrogen uptake, ΔN_{resom} : change in net N mineralisation due to a change in the soil organic N turnover time relative to the soil organic C turnover time; $\Delta NSOM$: change in net N mineralisation due to a change in the organic N pool; ΔNNE change in the ecosystem N balance (sum of N increases from biological N fixation and atmospheric N deposition and N losses to leaching and gaseous emissions); ΔN_{inorg} : changes in the inorganic N pool. The error bars on observations denote ± 1 standard error.

279x361mm (300 x 300 DPI)

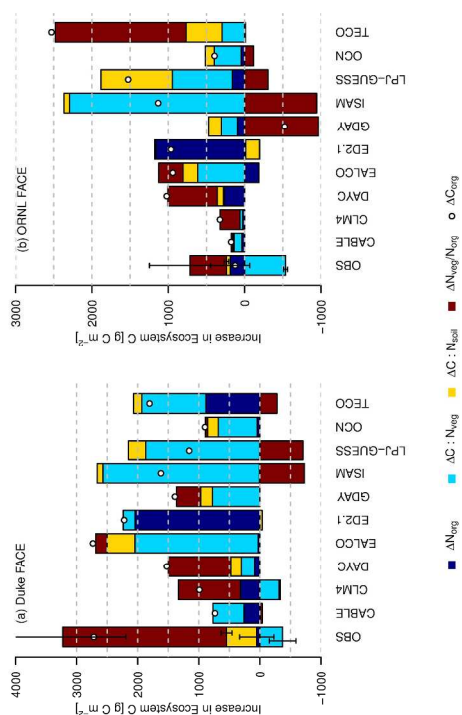


Figure 9: Total change in ecosystem C due to eCO₂ at the Duke (a) and ORNL (b) FACE sites resulting from changes in the total organic ecosystem N store (ΔN_{org}), vegetation and soil C:Ns ($\Delta C:N_{veg}$ and $\Delta C:N_{soil}$), as well as changes in the fractionation of total ecosystem N between vegetation and soil, measured as the fraction of total ecosystem N in vegetation ($f_{veg} = N_{veg}/N_{org}$). The error bars denote ± 1 standard error.
279x361mm (300 x 300 DPI)